

RECEIVED
APR 26 2000
OSTI

IS-T 1882

Kinetics and Mechanism of the Oxidation of Alkenes and Silanes
by Hydrogen Peroxide Catalyzed by Methylrhenum Trioxide (MTO)
and a Novel Application of Electrospray Mass Spectrometry to
Study the Hydrolysis of MTO

by

Tan, Haisong

PHD Thesis submitted to Iowa State University

Ames Laboratory, U.S. DOE

Iowa State University

Ames, Iowa 50011

Date Transmitted: November 8, 1999

PREPARED FOR THE U.S. DEPARTMENT OF ENERGY

UNDER CONTRACT NO. W-7405-Eng-82.

DISCLAIMER

This report was prepared as an account of work sponsored by an agency of the United States Government. Neither the United States Government nor any agency thereof, nor any of their employees, makes any warranty, express or implied, or assumes any legal liability or responsibility for the accuracy, completeness or usefulness of any information, apparatus, product, or process disclosed, or represents that its use would not infringe privately owned rights. Reference herein to any specific commercial product, process, or service by trade name, trademark, manufacturer, or otherwise, does not necessarily constitute or imply its endorsement, recommendation, or favoring by the United States Government or any agency thereof. The views and opinions of authors expressed herein do not necessarily state or reflect those of the United States Government or any agency thereof.

This report has been reproduced directly from the best available copy.

AVAILABILITY:

To DOE and DOE contractors: Office of Scientific and Technical Information
P.O. Box 62
Oak Ridge, TN 37831

prices available from: (615) 576-8401
FTS: 626-8401

To the public: National Technical Information Service
U.S. Department of Commerce
5285 Port Royal Road
Springfield, VA 22161

DISCLAIMER

Portions of this document may be illegible in electronic image products. Images are produced from the best available original document.

Kinetics and mechanism of the oxidation of alkenes and silanes by hydrogen peroxide catalyzed by methylrhenium trioxide (MTO) and a novel application of electrospray mass spectrometry to study the hydrolysis of MTO

Haisong Tan

Major Professors: James H. Espenson and Robert S. Houk

Iowa State University

Conjugated dienes were oxidized by hydrogen peroxide with methylrhenium trioxide as catalyst. As is true for other MTO-catalyzed reactions, methylrhenium bis-peroxide ($\text{CH}_3\text{Re}(\text{O})(\eta^2\text{-O}_2)_2(\text{H}_2\text{O})$) was the major reactive catalyst present. The rate constants between it and the dienes increase or decrease as substituents add or remove electron density from the double bond, suggesting a concerted mechanism in which the peroxide oxygen attacks the double bond electrophilically. The $\text{H}_2\text{O}_2/\text{MTO}$ oxidation system was also used in the regioselective cyclization of hydroxyalkenes to tetrahydrofurans and unsaturated carboxylic acids to lactones. In these reactions MTO acts as a bifunctional catalyst for both epoxidation and cyclization reactions. The reactions of trisubstituted silane with hydrogen peroxide catalyzed by MTO result in its quantitative conversion to silanol. An oxene mechanism is proposed for this reaction based on the kinetics and isotope ratio study.

The full kinetics pH profile for the base-promoted decomposition of MTO to CH_4 and ReO_4^- was examined with the inclusion of new data at pH 7-10. Spectroscopic and kinetics data gave evidence for mono- and dihydroxo complexes: $\text{MTO}(\text{OH}^-)$ and $\text{MTO}(\text{OH}^-)_2$. Some kinetic data were acquired with electrospray mass spectrometry to monitor the build up in the concentration of perrhenate ions.

TABLE OF CONTENTS

GENERAL INTRODUCTION	1
Introduction	1
Dissertation Organization	3
References	3
 CHAPTER I. KINETICS AND MECHANISM OF THE SI-H BOND O-ATOM INSERTION WITH HYDROGEN PEROXIDE CATALYZED BY METHYLTRIOXORHENIUM	 5
Introduction	5
Experimental Section	6
Results	7
Discussion	11
Supporting Information	18
References	19
 CHAPTER II. KINETICS AND MECHANISM OF THE DIHYDROXYLATION AND EPOXIDATION OF CONJUGATED DIENES WITH HYDROGEN PEROXIDE CATALYZED BY METHYL RHENIUM TRIOXIDE	 21
Abstract	21
Introduction	22
Experimental Section	23
Results	24
Discussion	33
Supporting Information	41
References	45

CHAPTER III. REGIOSELECTIVE OXIDATIVE CYCLIZATION OF HYDROXYALKENES TO TETRAHYDROFURANS CATALYZED BY METHYLTRIOXORHENIUM	47
Abstract	47
Introduction	47
Results and Interpretation	48
Experimental Section	54
Supporting Information	55
References	60
 CHAPTER IV. REGIOSELECTIVE HYDROXYLACTONIZATION OF γ,δ-UNSATURATED CARBOXYLIC ACIDS WITH HYDROGEN PEROXIDE CATALYZED BY METHYLTRIOXORHENIUM	 63
Abstract	63
Introduction	63
Results and Discussion	64
Experimental Section	68
Supporting Information	69
References	71
 CHAPTER V. BASE HYDROLYSIS OF METHYLTRIOXORHENIUM. THE MECHANISM REVISED AND EXTENDED: A NOVEL APPLICATION OF ELECTROSPRAY MASS SPECTROMETRY	 73
Abstract	73
Introduction	74
Experimental Section	76
Results	77
Discussion	79

References	86
GENERAL CONCLUSIONS	88
ACKNOWLEDGMENTS	90

GENERAL INTRODUCTION

Introduction

Methylrhenium trioxide (MTO) was first prepared in 1979,¹ but only in 1991 did Herrmann and co-workers recognize its potential in catalyst.² Since then more and more advantages of this catalyst have been realized. MTO is an attractive catalyst for activating hydrogen peroxide which is considered to be an environmentally "green" oxidant. MTO is soluble and stable in many solvents including water, stable towards high concentrations of acid (pH 0-3), air stable, easily purified by sublimation and recrystallization, and employable either homogeneously or heterogeneously.³ Until now the H₂O₂/MTO system has been shown to clearly catalyze the oxidation of alkenes,⁴⁻⁶ alkynes,⁷ alkyl and aryl sulfides,⁸ anilines,⁹ fullerenes,¹⁰ silanes¹¹ and phosphines.¹²

Compounds containing the silanol group are well known not only in nature, but also in industrial processes. The methods for selective preparation of silanols are limited due to the dimerization of silanol with trace acid or base. Silane can be quantitatively converted to the corresponding silanols upon treatment with H₂O₂/MTO. MTO has been found to activate H₂O₂ by formation of a bidentate monoperoxide, CH₃Re(O)₂(η -O₂), A, and a bisperoxide, CH₃Re(O)(η -O₂)₂(H₂O), B. Under the conditions of hydrogen peroxide present in large excess, usually B was the major reactive catalyst. Plotting rate constants vs total Taft value produced the linear relationship for the alkyl substituents as shown in Chapter I. The negative slope implies an electrophilic attack on the Si-H bond by catalyst B. The difference of the activation energy between experiment and calculation data comes from the solvent effect.

Conjugated dienes are important because useful compounds are derived from their epoxidation and dihydroxylation reactions. $\text{H}_2\text{O}_2/\text{MTO}$ is a very efficient system to oxidize diene to epoxide and diol. The rate constant between catalyst B and the dienes was studied to explore the structural and electronic features of the mechanism which govern the rates and products. Many of the products are diols, except when the carbocation intermediates for epoxide ring opening are so unstable to prolong their lives. When urea-hydrogen was used instead of 30% hydrogen peroxide water solution, the monoperoxides were obtained. The detail of this study is given in Chapter II.

A number of natural products, such as polyether antibiotics, contain tetrahydrofuran rings. Certain metal catalysts have been developed in recent years to synthesize these heterocycles. However these metal catalyst must be taken stoichiometrically and the yields of furan are only 50-70%. We have found that MTO functions as an efficient catalyst with hydrogen peroxide to make tetrahydrofurfuryl alcohols from 5-hydroxy alkenes. This method achieves nearly complete regioselectivity as described in Chapter III.

Functionalized γ -lactones serve as chiral building blocks in natural products synthesis. Heteroatom cyclizations lead to γ -lactones and allows two neighboring chiral centers to be introduced and concurrent. Cyclization of carboxylic acids and esters have been widely studied, but with unsatisfactory yields. Treatment of γ,δ -unsaturated carboxylic acid and esters with H_2O_2 affords δ -hydroxy- γ -lactones in a single high-yield step at room temperature when MTO is used as a catalyst. Investigation of these reactions are present in Chapter IV.

The base hydrolysis kinetics of methylrhenium trioxide (MTO) was reported by Herrmann's group (at low pH) and our group (at high pH) in 1996. Both groups agreed that the exclusive products are methane and perrhenate ions.

However the rate constants thus assigned could not be reconciled with one another, and differed by more than four orders of magnitude. The goal of our study is to obtain kinetic data that cover the full pH range and to formulate a single mechanism to describe all the data. The reaction kinetics study at intermediate pH values with UV-Vis and electrospray mass spectrometric (ES-MS) techniques is described in Chapter V.

Dissertation Organization

This dissertation consists of five chapters. The first four chapters deal with the oxidation of alkenes and silanes by $\text{H}_2\text{O}_2/\text{MTO}$. Chapter I has been submitted for publication. Chapter II has already been published in *Inorganic Chemistry*. Chapter III and IV have been submitted for publication in *Journal of Molecular Catalysis*. The last chapter deals with base hydrolysis of MTO which has been published in *Inorganic Chemistry*. Each section is self contained with its own equations, tables, figures and references. Following the last chapter are some general conclusions. All the work in this dissertation was performed by this author.

References

- (1) Beattie, I. R.; Jones, P. J. *Inorg. Chem.* **1979**, *18*, 2318.
- (2) Herrmann, W. A.; Fischer, R. W.; Scherer, W.; Rauch, M. U. *Angew. Chem., Int. Ed. Engl.* **1993**, *32*, 1157.
- (3) Abu-Omar, M.; Hansen, P. J.; Espenson, J. H. *J. Am. Chem. Soc.* **1996**, *118*, 4966.
- (4) Herrmann, W. A.; Fischer, R. W.; Rauch, M. U.; Scherer, W. J. *Mol. Catal.* **1994**, *86*, 243.
- (5) Al-Ajlouni, A.; Espenson, J. H. *J. Am. Chem. Soc.* **1995**, *117*, 9243.

- (6) Al-Ajlouni, A.; Espenson, J. H. *J. Org. Chem.* **1996**, *61*, 3969.
- (7) Zhu, Z; Espenson, J. H. *J. Org. Chem.* **1995**, *60*, 7728.
- (8) Vassell, K. A.; Espenson, J. H. *Inorg. Chem.* **1994**, *33*, 5491.
- (9) Zhu, Z; Espenson, J. H. *J. Org. Chem.* **1995**, *60*, 1326.
- (10) Murray, R. W.; Lyannar, K. *Tetrahedron Lett.* **1997**, *38*, 335.
- (11) Tan, H.; Yoshikawa, A; Gordon, M. S.; Espenson, J. H. Manuscript in Preparation.
- (12) Abu-Omar, M.; Espenson, J. H. *J. Am. Chem. Soc.* **1995**, *117*, 272.

CHAPTER I

KINETICS AND MECHANISM OF THE SI-H BOND O-ATOM INSERTION
WITH HYDROGEN PEROXIDE CATALYZED BY METHYLRHENIUM TRIOXIDE

Haisong Tan, James H. Espenson, Akihiko Yoshikawa, Mark S. Gordon

Introduction

Compounds containing the silanol group are well known not only in nature, but also in industrial processes in which polymeric materials such as polydimethylsiloxanes (silicones) and sol-gels are produced by condensation reactions of the reactive silanols. The methods for selective preparation of silanols are limited.¹ Sterically exposed silanols are very easy to dimerize with traces of acid or base. Currently one of the best methods of making silanols is the oxidation of silanes with dioxiranes, but the disadvantage is that this reagent should be used stoichiometrically and at low temperature (-20-0 °C).² Catalytic Si-H bond O-atom insertion with hydrogen peroxide has also been reported for Ti-beta zeolite, but this reaction needs 85% H₂O₂ and a special Ti-beta-Na zeolite catalyst.³

Methylrhenium trioxide (MTO) is an effective catalyst for the addition of an O atom to a number of substrates⁴⁻¹⁰, but C-H oxidation reactions are quite sluggish. We have turned to Si-H reactions to explore this issue. The reactions of trisubstituted silane R₃SiH with hydrogen peroxide catalyzed by MTO result in its quantitative conversion to R₃SiOH. High and stable yield of silanols was achieved by replacing 30% hydrogen peroxide with urea-hydrogen peroxide. When this work was in process, we noted a reference of using MTO and urea-hydrogen peroxide to oxidize silane to silanol selectively.¹¹

Experimental Section

Materials. Deuterated acetonitrile was used as the solvent for quantitative kinetic studies (Cambridge Isotope Lab.). Silanes and methylrhenium trioxide were purchased (Aldrich). Tri-n-butylsilane-d was prepared following literature procedure.¹² Solutions of CH_3ReO_3 in CD_3CN were stored at 5°C and used within 3 days.

^1H and ^{13}C NMR spectra were obtained from Varian VXR-300 or Bruker DRX-400 spectrometers. Chemical shifts were referenced to Me_4Si . A GC (Varian 3400)/MS (Finnegan TSQ 700 triple quadrupole) spectrometer was used for certain product studies.

Kinetics. Kinetics determinations were carried out in CD_3CN at $25.0 \pm 0.2^\circ\text{C}$ on Bruker DRX-400 NMR spectrometer. The kinetics data were obtained by following the loss of silane signal in NMR spectra. The experiments used 0.20-0.80 M H_2O_2 , 0.010M silanes, 2-8 mM MTO and 10% total H_2O in CD_3CN . Reaction mixtures were prepared in NMR tube with silanes added last.

Products. To identify the products, 0.20 mmol of silane was added to an NMR tube containing 6 μmol MTO, 0.5 mmol urea-hydrogen peroxide in 1.0 mL CD_3CN , which was held at room temperature for several hours. The products were characterized by their ^1H and ^{13}C NMR spectra and by MS. Since all the products are known materials, it suffices to present the results in the Supporting Information.

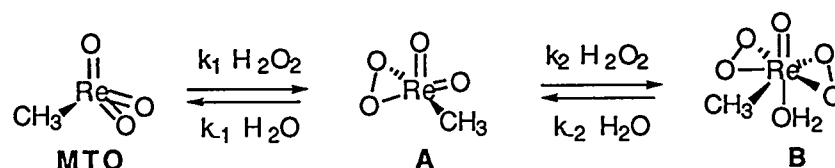
Computational Methods. Calculations for the transition state employ the GAMESS program.¹³ Effective core potentials (ECPs) and valence basis sets (VBSs)¹⁴ are used for heavy atoms and a -31G basis for H. The effective core potentials of Steven et al.¹⁴ (SBK) are derived from numerical Dirac-Hartree-Fock (DHF) calculations on atoms for all elements larger than neon and thus

implicitly include the Darwin and mass-velocity relativistic effects. Spin-orbit coupling is averaged out in potential generation.¹⁵ Geometries are optimized at the restricted Hartree-Fock (RHF) level for closed-shell singlets. Enthalpic data are determined using Møller-Plesset second-order perturbation theory (MP2) energies at RHF-optimized geometries with zero point energy and temperature corrections (to 298.15 K).

Results

The mechanism of MTO-catalyzed reactions have been thoroughly documented.¹⁶⁻¹⁹ The active forms of MTO are its monoperoxo and diperoxo complexes, designated A and B, respectively (Scheme 1).

Scheme 1



In accord with earlier findings, both A and B react with the substrate. Their respective second-order rate constants are k_3 and k_4 , eqs 1 and 2.



The rate law for product buildup, assuming the improved steady-state approximation, can be derived.⁹ To simplify the treatment implied by the complete equation, conditions were set to attain the limiting form. When the concentration of silane (0.010 M) was much lower than the concentration of hydrogen peroxide (0.50 M), data are more informative as to the oxygen-transfer

step of the reaction. The experiments were done with 10% water and 2.0-8.0 mM of MTO. MTO always mixed with hydrogen peroxide first before adding silane. Under these conditions, the limiting form becomes

$$-\frac{d[S]}{dt} = \frac{d[P]}{dt} = k_4[Re]_T[S] \quad (4)$$

S is representing silane and P is product silanol. The rate constant obtained (k_ψ) is expected to be a linear function of $[Re]_T$, but not expected to show any dependence on $[H_2O_2]$. Figure 1 confirms the linearity of the variation for two silanes, triisopropylsilane and dimethylphenylsilane. From the slopes of the lines, the respective values of k_4 are 0.1000 ± 0.0006 and 0.0500 ± 0.0004 . Another experiment shows that the k_ψ has no dependence on the concentration of hydrogen peroxide varied from 0.20 to 0.80 M. The rate constants so determined for 10 silanes are presented in Table 1.

Activation Parameters. The changes of k_4 with temperature (0 - 50 °C) for both triethylsilane and tri-n-butylsilane were studied. Analysis by the Transition State Theory (TST) equation

$$\ln\left(\frac{k_4}{T}\right) = \ln\left(\frac{R}{Nh}\right) + \frac{\Delta S^\ddagger}{R} - \frac{\Delta H^\ddagger}{RT} \quad (5)$$

gave triethylsilane: $\Delta H^\ddagger = 11.8 \pm 0.4$ kcal mol⁻¹, and $\Delta S^\ddagger = -22.6 \pm 1.6$ cal mol⁻¹ K⁻¹ and tributylsilane: $\Delta H^\ddagger = 12.4 \pm 0.1$ kcal mol⁻¹, and $\Delta S^\ddagger = -20.6 \pm 0.3$ cal mol⁻¹ K⁻¹. The activation energy calculated from Arrhenius equation are 12.4 ± 0.4 kcal mol⁻¹ for triethylsilane and 13.0 ± 0.1 kcal mol⁻¹ for tributylsilane.

Products. We used ¹H NMR, ¹³C NMR, and MS to identify the reaction products. They are also shown in each case in Table 1, along with the reaction yields. When the hydrogen peroxide was used, the concentration of disiloxane

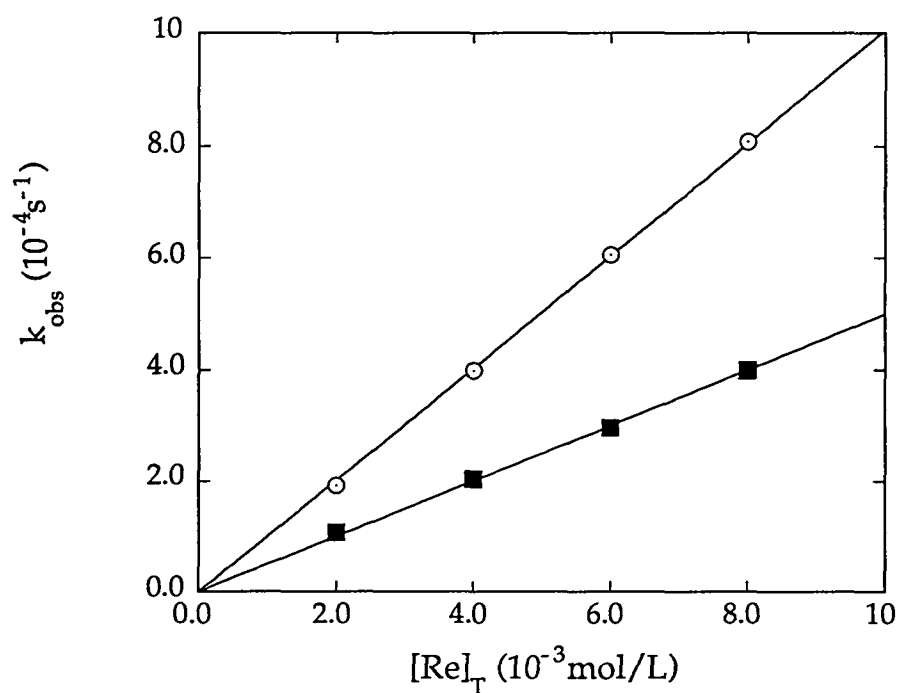


Figure 1. Pseudo-first-order rate constants for the oxidation reactions of triisopropylsilane and dimethylphenylsilane (each 10 mM) by hydrogen peroxide (0.50 M) in acetonitrile containing 10% water varying linearly with the total rhenium concentration.

Table 1. Rate Constants and Products for the MTO-Catalyzed Oxidation of Silane by Hydrogen Peroxide

Entry	Reactants	k_4 (M ⁻¹ S ⁻¹) ^a	Products	% Yield ^b
1	EtMe ₂ SiH	0.110	EtMe ₂ SiOH ^c	80
2	t-ButMe ₂ SiH	0.100	t-ButMe ₂ SiOH	94
3	Et ₃ SiH	0.103	Et ₃ SiOH	94
4	Pr ₃ SiH	0.131	Pr ₃ SiOH	97
5	i-Pr ₃ SiH	0.100	i-Pr ₃ SiOH	98
6	n-But ₃ SiH	0.167	But ₃ SiOH	97
7	(n-C ₆ H ₁₃) ₃ SiH	0.171	(n-C ₆ H ₁₃) ₃ SiOH	96
8	PhMe ₂ SiH	0.050	PhMe ₂ SiOH ^c	82
9	Ph ₂ MeSiH	0.0224	Ph ₂ MeSiOH	95
10	Ph ₃ SiH	0.0217	Ph ₃ SiOH	98

^a k_4 was measured in CD₃CN with MTO/30% H₂O₂.

^b Yield was measured in CD₃CN with MTO/Urea-H₂O₂ and based on ¹H NMR or GC peak integrations.

^c The solvent is CDCl₃.

increased with time after the oxidation reaction. This is due to the decomposition of MTO to perhenic acid which can catalyze the dimerization of silane. To confirm this result, 0.010 M HReO_4 was added to 0.20 M Et_3SiOH in acetonitrile. After an hour, most of Et_3SiOH changed to $\text{Et}_3\text{SiOSiEt}_3$. In an attempt to minimize disiloxane formation, a solid reagent urea-hydrogen peroxide (UHP, $\text{H}_2\text{NC(O)NH}_2 \cdot \text{H}_2\text{O}_2$) was used without any addition of water to the acetonitrile. Under this condition, most of the silane gave high yield of silanol, Table 1. The two exceptions are dimethylethylsilane and dimethyl phenylsilane. These two compounds have relatively small substituents which make the dimerization of silanol much easier. In acetonitrile, the products are mixtures of silanol and disiloxane with UHP. When the solvent was changed to chloroform, the yield of silanols increased to 80%.

Discussion

Previous data have shown that substituents have a regular effect on the rate, depending on the direction in which they alter the electron density at the Si-H bond. Figure 2 shows the logarithm of the rate constant as a function of the Si-H stretching frequency. The deviant point is $i\text{-Pr}_3\text{SiH}$ which has the most bulky substituent group in our substrates. The near linear correlation and its sign are consistent with Si-H stretching being important in the reaction's rate-determining step. With the stronger bonds (those of higher frequency) the silanes have less reactivity.²⁰

Another correlation is to relate the rates to some type of Hammett σ value. However the Hammett equation is not successful for reactions of aliphatic compounds if the normal σ constants are used. Another substituent constants, Taft σ^* value, was used to allow the extension of the method to such systems.²¹

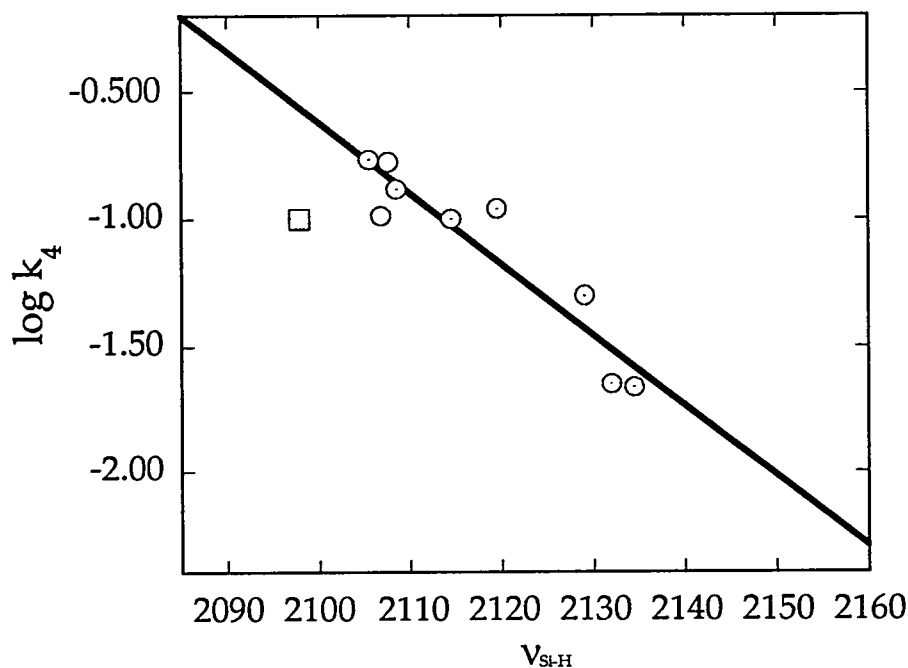


Figure 2. Logarithm of the rate constants of silane oxidation as a function of the Si-H stretching frequency.

A summation of the σ^* values for all substituents ($\Sigma\sigma^*$) was taken as indicative of the silicon's total electronic environment.²² Plotting $\Sigma\sigma^*$ vs the rate k_4 produced the linear relationship for the alkyl substituents (Figure 3). The correlation implies a direct interaction between the substituent and the reaction site. The slope of the plot ρ , representing a reaction parameter, is -0.39. Its negative value denotes electrophilic attack on the reaction site by catalyst B. Since silicon is relatively electropositive, an electrophilic attack by B seems unlikely.

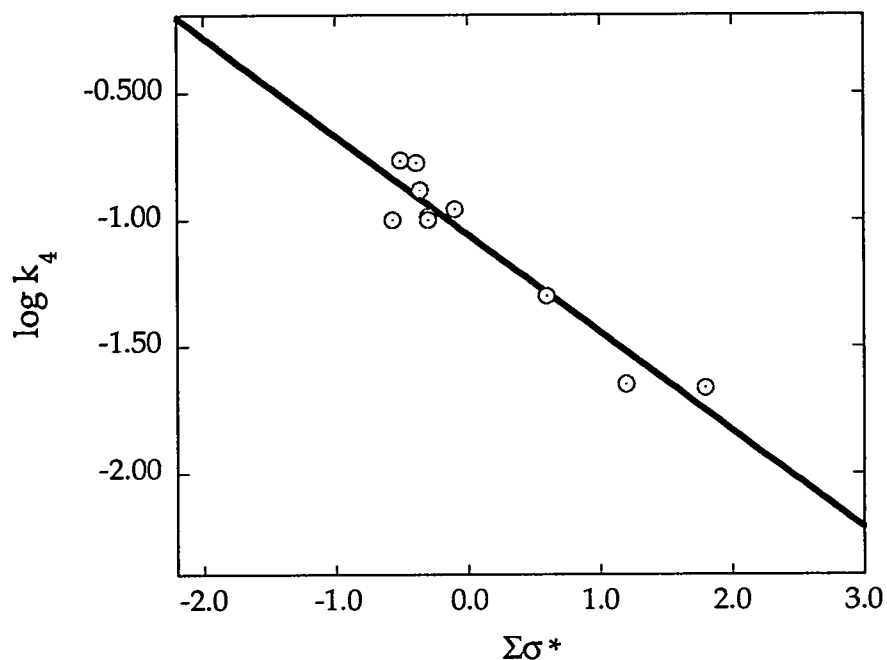


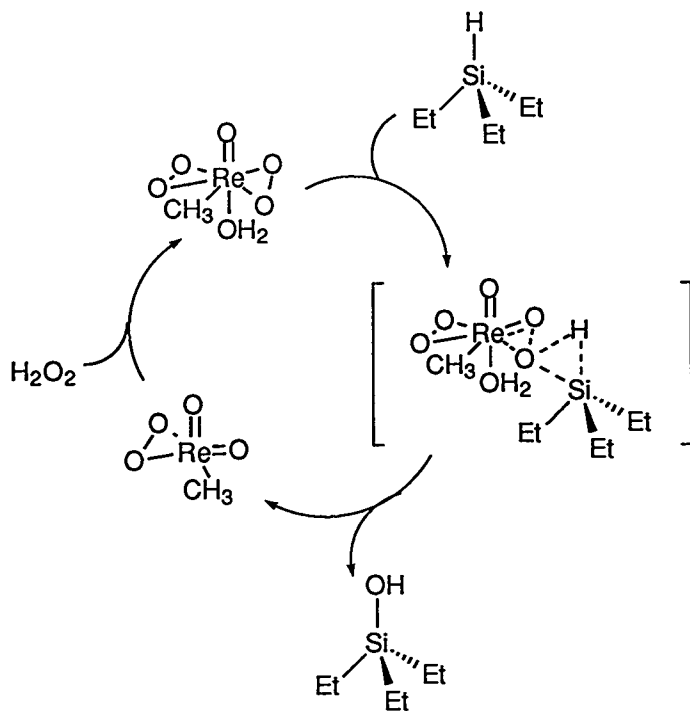
Figure 3. Correlation of the rate constants ($\log k_4$) for the silane oxidation with the total Taft value of each silane.

The hydrogen bound to silicon is hydridic and is the likely site on attack by an electrophile. If attack by B on the Si-H bond occurs in the rate controlling step, then a primary deuterium isotope effect is predicted. The deuterium isotope effect, $k_H/k_D = 2.1$ at 0 °C, was determined for the reaction of tri(n-butyl)silane with MTO. This result is similar to that reported for the insertion of dichlorocarbene into nBut₃SiH ($k_H/k_D = 1.23$)²³ and the oxygen atom insertion into Et₃SiH by dioxirane ($k_H/k_D = 2.6$).² Therefore, as for the carbene insertions,

an oxene mechanism is proposed for the oxidation of silane by compound **B** (Scheme 2).

The activation parameters for k_4 support this model. The value of ΔS^\ddagger is negative which reflects the bimolecular reactions. The high value of ΔH^\ddagger need a composite of bond breaking (Re-O, O-O) and bond making (Si-O) in the reaction, otherwise the reaction would be extraordinarily slow.

Scheme 2



Further evidence for the reaction scheme comes from the calculation of the transition state. Selected metric data for the transition state of triethylsilane are collected in Table 2 and Figure 4. Compound **A** is used instead of compound **B** to simplify the calculation, which will not affect the result because of the compatibility of the rate constant for **A** (k_3) with that of **B** (k_4). From Figure 4 we can see that an oxygen atom is partially inserted into Si-H bond from catalyst **A**,

Table 2. Calculated data for the reaction of triethylsilane.

Compound	Bond	Bond Length (Å)	Bond	Bond Length (Å)
CH ₃ Re(O ₂)O ₂	Re(1) - C(2)	2.131	Re(1) - O(8)	1.653
	Re(1) - O(6)	1.909	Re(1) - O(9)	1.880
	Re(1) - O(7)	1.653	O(6) - O(9)	1.395
HSiEt ₃	Si(1) - H(2)	1.500	Si(1) - C(4)	1.904
	Si(1) - C(3)	1.904	Si(1) - C(5)	1.898
Transition State	Re(1) - C(2)	2.120	Si(10) - H(11)	1.537
	Re(1) - O(6)	1.734	Si(10) - C(12)	1.894
	Re(1) - O(7)	1.663	Si(10) - C(13)	1.898
	Re(1) - O(8)	1.663	Si(10) - C(14)	1.898
	Re(1) - O(9)	2.161	Si(10) - O(9)	2.947
	O(6) - O(9)	1.928	O(9) - H(11)	1.528

just as the mechanism we proposed. Table 2 shows that the transition state bonds of Si(10)-H(11), Re(1)-O(9) and O(6)-O(9) are longer than that of the reactants, but Re(1)-O(6) bond is shorter because it will change back to the Re-O double bond after the reaction. The charge distribution on the peroxide oxygen (O(6) and O(9)) of compound A is more positive than that of O(7) and O(8) (Table 3), which can explain why it is peroxide oxygen that attacks Si-H bond electrophilically. In the transition state the charge distribution on O(9) becomes more positive during the electrophilic attack on Si-H bond. However O(6) is more negative and is starting to change back to Re-O double bond. The activation energy is 28.5 kcal mol⁻¹ from calculation, which is more than double of the experiment value that was collected in 10% H₂O-CD₃CN solvent. From Table 3 we can see that there are

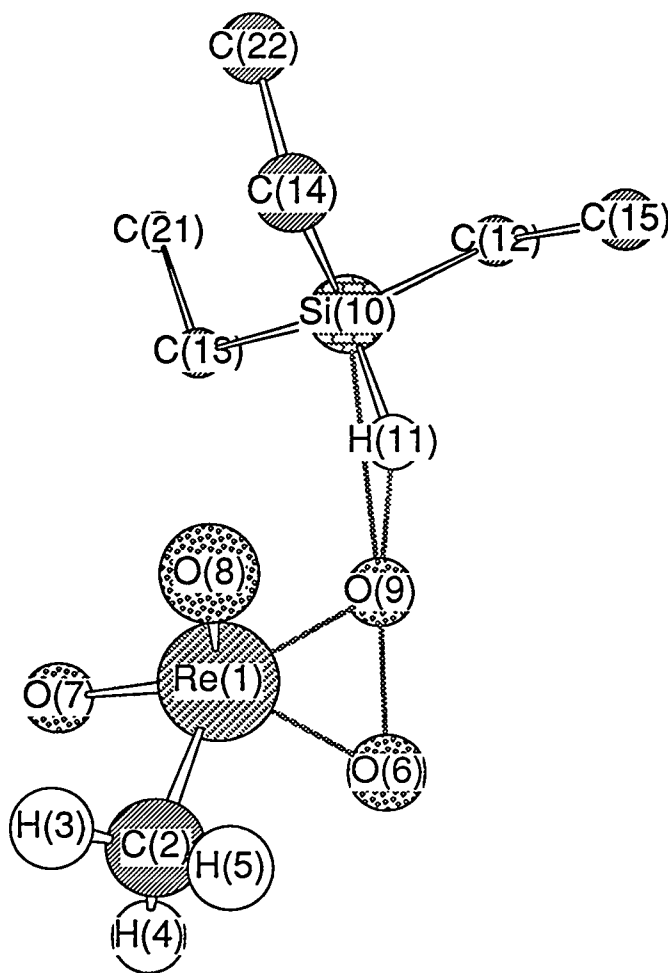


Figure 4. Calculated geometry of triethylsilane transition state.

more polar centers on the transition state than the triethylsilane. This will attract more polar solvent molecules in the H_2O - CD_3CN solution. The solvent molecules around will stabilize the transition state in the solution, which will decrease the transition state energy level and the reaction energy barrier in the solvent.

Table 3. Calculated charge distribution.

Compound	Atom	Charge Distribution	Atom	Charge Distribution
CH ₃ ReO ₃	Re(1)	1.597	H(5)	0.167
	C(2)	-0.111	O(6)	-0.662
	H(3)	0.167	O(7)	-0.662
	H(4)	0.167	O(8)	-0.662
CH ₃ Re(O ₂)O ₂	Re(1)	1.479	H(5)	0.160
	C(2)	-0.025	O(6)	-0.334
	H(3)	0.166	O(7)	-0.622
	H(4)	0.160	O(8)	-0.622
			O(9)	-0.362
HSiEt ₃	Si(10)	0.162	C(14)	-0.281
	H(11)	-0.056	C(15)	-0.137
	C(12)	-0.268	C(16)	-0.140
	C(13)	-0.256	C(17)	-0.152
Transition State	Re(1)	1.480	Si(10)	0.064
	C(2)	-0.040	H(11)	-0.045
	H(3)	0.163	C(12)	-0.272
	H(4)	0.170	C(13)	-0.243
	H(5)	0.170	C(14)	-0.248
	O(6)	-0.585	C(15)	-0.153
	O(7)	-0.637	C(21)	-0.133
	O(8)	-0.635	C(22)	-0.137
	O(9)	-0.291		

We conclude that the rate control step of MTO-catalyzed silane oxidation involves electrophilic attack by B on the Si-H bond. The Si-H stretching is important in the rate-determining step, with the stronger bonds (those of higher frequency) possessing less reactivity. Silanols are obtained with high yield when UHP is used instead of 30% hydrogen peroxide. The difference of the activation energy between experiment and calculation data comes from the solvent effect.

Acknowledgment. This research was supported by the U. S. Department of Energy, Office of Basic Energy Sciences, Division of Chemical Sciences under contract W-7405-Eng-82.

Supporting Information

NMR (in CD₃CN) and MS data

Ethyldimethylsilanol (1) ¹H NMR (in CD₃Cl), δ/ppm 0.93-0.99(t, 3H), 0.55-0.59(q, 2H), 0.12(s, 6H); ¹³C NMR (in CD₃Cl), δ/ppm 9.64, 6.82, -0.65. MS(EI): 103(M⁺-H, 100%), 89(15%), 87(25%).

tert-Butyldimethylsilanol (2) ¹H NMR, δ/ppm 0.87(s, 9H), 0.01(s, 6H); ¹³C NMR, δ/ppm 26.41, 18.94, -3.06. MS(EI): 131(M⁺-H, 10%), 117(6%), 75(100%).

Triethylsilanol (3) ¹H NMR, δ/ppm 0.90-0.96(t, 9H), 0.46-0.56(q, 6H); ¹³C NMR, δ/ppm 7.32, 6.81. MS(EI): 131(M⁺-H, 3%), 115(16%), 103(100%).

Tripropylsilanol (4) ¹H NMR, δ/ppm 1.33-1.40(m, 6H), 0.92-0.97(t, 9H), 0.51-0.55(m, 6H); ¹³C NMR, δ/ppm 18.98, 18.92, 17.78. MS(EI): 173(M⁺-H, 2%), 157(15%), 131(100%).

Triisopropylsilanol (5) ¹H NMR, δ/ppm 0.99-1.02(m, 21H); ¹³C NMR, δ/ppm 18.48, 13.54. MS(EI): 175(M+H⁺, 2%), 157(14%), 131(100%).

Tributylsilanol (6) ^1H NMR, δ/ppm 1.27-1.33(m, 12H), 0.85-0.89(t, 9H), 0.49-0.55(m, 6H); ^{13}C NMR, δ/ppm 27.83, 26.67, 16.05, 14.75. MS(EI): 217($\text{M}+\text{H}^+$, 2%), 199(6%), 159(100%).

Trihexylsilanol (7) ^1H NMR, δ/ppm 1.25-1.33(m, 24H), 0.85-0.89(t, 9H), 0.49-0.54(m, 6H); ^{13}C NMR, δ/ppm 34.64, 32.92, 24.44, 23.93, 16.45, 15.19. MS(EI): 283($\text{M}-\text{OH}^-$, 4%), 215(100%).

Dimethylphenylsilanol (8) ^1H NMR (in CD_3Cl), δ/ppm 7.60-7.63(m, 2H), 7.39-7.41(m, 3H), 0.42(s, 6H); ^{13}C NMR (in CD_3Cl), δ/ppm 139.31, 133.25, 129.84, 128.10, 0.16 MS(EI): 151(M^+-H , 4%), 137(100%).

Dimethylphenylsilanol (9) ^1H NMR, δ/ppm 7.60-7.63(m, 4H), 7.36-7.41(m, 6H), 0.60(s, 3H); ^{13}C NMR, δ/ppm 139.60, 135.02, 130.84, 118.68, -0.75 MS(EI): 214(M^+ , 27%), 199(100%).

Triphenylsilanol (10) ^1H NMR, δ/ppm 7.58-7.62(m, 6H), 7.36-7.45(m, 9H); ^{13}C NMR, δ/ppm 137.44, 135.95, 131.18, 129.16 MS(EI): 276(M^+ , 95%), 199(100%).

References

- (1) Lickiss, P. D. *Adv. Inorg. Chem.* **1995**, 42, 147.
- (2) Adam, W.; Mello, R.; Curci, R. *Angew. Chem., Int. Ed. Engl.*, **1990**, 29, 890.
- (3) Adam, W.; Garcia, H.; Mitchell, C. M.; Saha-Möller, C. R.; Weichold, O. *J. Chem. Soc., Chem. Comm.* **1998**, 2609
- (4) Herrmann, W. A.; Fischer, R. W.; Scherer, W.; Rauch, M. U. *Angew. Chem., Int. Ed. Engl.* **1993**, 32, 1157.
- (5) Zhu, Z.; Espenson, J. H. *J. Org. Chem.* **1995**, 60, 1326.
- (6) Zhu, Z.; Espenson, J. H. *J. Am. Chem. Soc.* **1995**, 117, 272.
- (7) Al-Ajlouni, A.; Espenson, J. H. *J. Org. Chem.* **1996**, 61, 3969.

- (8) Rudolph, J.; Reddy, K. L.; Chiang, J. P.; Sharpless, K. B. *J. Am. Chem. Soc.* **1997**, *119*, 6189.
- (9) Tan, H.; Espenson, J. H. *Inorg. Chem.* **1998**, *37*, 467.
- (10) Zauche, T. H.; Espenson, J. H. *Inorg. Chem.* **1998**, *37*, 6827.
- (11) Adam, W.; Mitchell, C. M.; Saha-Möller, C. R.; Weichold, O. *J. Am. Chem. Soc.* **1999**, *121*, 2097.
- (12) Brookhart, M.; Grant, B. E. *J. Am. Chem. Soc.* **1993**, *115*, 2151.
- (13) Schmidt, M. W.; Baldrige, K. K.; Boatz, J. A.; Elbert, S. T.; Gordon, M. S.; Jensen, J. H.; Koseki, S.; Matsunaga, N.; Nguyen, K. A.; Su, S. J.; Windus, T. L.; Dupuis, M.; Montgomery, J. A. *J. Comp. Chem.* **1993**, *14*, 1347.
- (14) Stevens, W. J.; Basch, H. B.; Krauss, M.; Jasien, P. G. *Can. J. Chem.* **1992**, *70*, 612.
- (15) Cundari, T. R.; Snyder, L. A.; Yoshikawa, A. *J. Mol. Struct.* **1998**, *425*, 13.
- (16) Espenson, J. H.; Abu-Omar, M. M. *Adv. Chem. Ser.* **1997**, *253*, 99.
- (17) Gable, K. P. *Adv. Organomet. Chem.* **1997**, *41*, 127.
- (18) Herrmann, W. A.; Kühn, F. E. *Acc. Chem. Res.* **1997**, *30*, 169.
- (19) Romão, C. C.; Kühn, F. E.; Herrmann, W. A. *Chem. Rev.* **1997**, *97*, 3197.
- (20) Spialter, L.; Swansiger, W. *J. Am. Chem. Soc.* **1968**, *90*, 2187.
- (21) Espenson, J. H. *Chemical Kinetics and Reaction Mechanisms*, 2d Ed.; page 229; McGraw-Hill, Inc.: New York, 1995.
- (22) Spialter, L.; Pazdernik, L.; Bernstein, S.; Swansiger, W.; Buell, G.; Freeburger, M. *J. Am. Chem. Soc.* **1971**, *93*, 5682.
- (23) Spialter, L.; Swansiger, W.; Pazdernik, L.; Freeburger, M. *J. Organomet. Chem.* **1971**, *27*, C25.

CHAPTER II

KINETICS AND MECHANISM OF THE DIHYDROXYLATION AND
EPOXIDATION OF CONJUGATED DIENES WITH HYDROGEN PEROXIDE
CATALYZED BY METHYLRHENIUM TRIOXIDE

A paper published in *Inorganic Chemistry* *

Haisong Tan and James H. Espenson

Abstract

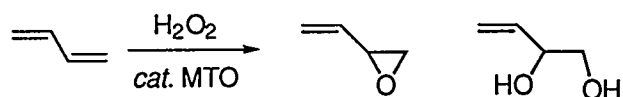
The title reactions occur readily. With acetonitrile chosen as the solvent, 17 of them were studied by kinetic methods. As is true for other MTO-catalyzed reactions, peroxorhenium complexes are the active species. Under the conditions of hydrogen peroxide present in large excess, usually employed here, $\text{CH}_3\text{Re}(\text{O})(\eta^2\text{-O}_2)_2(\text{OH}_2)$ was the major reactive catalyst present. The rate constant between it and the dienes increase or decrease as substituents add or remove electron density from the C=C bonds, suggesting a concerted mechanism in which the double bond attack a peroxide oxygen. Many of the products are diols, some rearranged, except when the stability of carbocation intermediates for epoxide ring opening are so unstable as to prolong their lives. When urea-hydrogen peroxide was used instead, the monoepoxides were obtained.

* Tan, H.; Espenson, J. H. *Inorg. Chem.* 1998, 37, 467.

Introduction

Theoretical interest and the practical importance of the epoxidation of olefins have generated sustained efforts in this area. Any number of catalysts effect epoxidations, those of greatest interest here being high-valent metal oxo compounds that activate hydrogen peroxide.¹⁻⁶ A new catalyst, methylrhenium trioxide (CH_3ReO_3 , abbreviated as MTO), first found important application in epoxidation reactions based on hydrogen peroxide as the oxidizing agent.^{7,8} Since that time, quantitative studies of the MTO-catalyzed reactions have been carried out to define in some detail the steps and intermediates in the epoxidation mechanism^{9,10} and other work has sought to improve the selectivity for epoxides.¹¹

Conjugated dienes are important because useful compounds are derived from their epoxidation and dihydroxylation reactions. Conceptually, this can be represented by eq 1, showing the parent 1,3-butadiene as the reactant.



We have investigated 16 analogous compounds, and have explored the structural and electronic features of the mechanism that govern the rates and products. Our search of the literature did reveal earlier work on catalytic diene epoxidations,¹²⁻¹⁶ but no earlier catalytic system in which the kinetics of epoxide (oxirane) formation from dienes and hydrogen peroxide had been studied systematically.

Most of the reactions gave the generally-less-desired diols, a consequence of epoxide ring-opening reactions under the reaction conditions brought about by the water present in 30% hydrogen peroxide. Consequently, we replaced hydrogen peroxide with urea-hydrogen peroxide, $\text{H}_2\text{NC(O)NH}_2 \cdot \text{H}_2\text{O}_2$,

abbreviated as UHP. This reagent is insoluble and thus unsuited for kinetics, but it gave the epoxides in good yield.

Experimental Section

Materials. Acetonitrile was used as the solvent for quantitative kinetic studies (HPLC-grade, Fisher). Dienes and methylrhenium trioxide were purchased (Aldrich). Solutions of CH_3ReO_3 in CH_3CN were stored at 5°C and used within 3 days. Hydrogen peroxide solutions were made by diluting the 30% material with acetonitrile; dilute solutions were discarded after three hours. High purity water was obtained by passing laboratory distilled water through a Millipore-Q water purification system.

^1H and ^{13}C NMR spectra were obtained from Varian VXR-300 or Bruker DRX-400 spectrometers. Chemical shifts were referenced to Me_4Si . A GC (Varian 3400)/MS (Finnigan TSQ 700 triple quadrupole) spectrometer was used for certain product studies.

Kinetics. Kinetics determinations were carried out in CH_3CN at $25.0 \pm 0.2^\circ\text{C}$. Quartz cuvettes with different optical paths of 0.01–0.2 cm were used. The kinetics data were obtained by following the loss of diene absorption in the region 230–260 nm using a Shimadzu UV-visible spectrometer. The experiments used 0.004–0.50 M H_2O_2 , 0.2–20 mM diene, 0.1–20 mM MTO generally but as high as 100 mM in one very slow reaction, and 0.0176–2.2 M H_2O . Reaction mixtures were prepared in a spectrophotometric cell with the last reagent added being either H_2O_2 (Method I) or the diene (Method II) to optimize the kinetic conditions as explained later.

The absorbance-time curves were analyzed by pseudo-first-order or initial rate methods. The pseudo-first-order rate constants (k_{p}) were evaluated by

nonlinear least-squares fitting of the absorbance-time profiles to a single exponential equation:

$$\text{Abs}_t = \text{Abs}_\infty + (\text{Abs}_0 - \text{Abs}_\infty) \times \exp(-k_\psi t) \quad (1)$$

For Method I, the initial rate method was used. The concentration of the product was calculated from the absorbance at each time. The equation is

$$[\text{diene}]_t = [\text{diene}]_0 \times \frac{\text{Abs}_t - \text{Abs}_\infty}{\text{Abs}_0 - \text{Abs}_\infty} \quad (2)$$

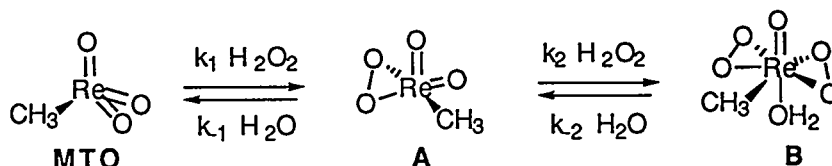
The concentration-time data were then fit to a power series, $C_t = m_0 + m_1t + \dots + m_nt^n$, with the program KaleidaGraph. Differentiation shows that the value of m_1 is the initial rate. Between 4–9 terms were used in the series, the choice being largely immaterial. Initial rates are less precise, but they are particularly useful when a complex kinetics pattern invalidates a simpler treatment.

Products. To identify the products, 0.30 mmol of diene was added to an NMR tube containing 6 μmol MTO, 1.2 mmol H_2O_2 , and 5.3 mmol water in 0.6 mL CD_3CN , which was held at room temperature for 2 hours. If a complex mixture was formed, the major products were separated by TLC; in most cases this step was unnecessary. The products were characterized by their ^1H and ^{13}C NMR spectra and by GC-MS. Since most of these products are known materials, it suffices to present the results in the Supporting Information.

Results

It has been well documented that two peroxorhenium compounds exist in equilibrium with MTO and hydrogen peroxide.¹⁷ The species are depicted in **Scheme 1**, where they are designated **A** and **B**. These species have proved responsible for the O-atom transfer reactions of MTO–hydrogen peroxide.

Scheme 1



The equilibrium constants are markedly dependent on the water concentration. Two sets of values of $K/L \text{ mol}^{-1}$ will be cited, in 1:1 $\text{CH}_3\text{CN}-\text{H}_2\text{O}$ at pH 1,¹⁸ $K_1 = 1.3 \times 10^1$, $K_2 = 1.36 \times 10^2$; in CH_3CN containing 2.6 M H_2O , $K_1 = 2.1 \times 10^2$, $K_2 = 6.6 \times 10^2$.¹⁹ As reported in related instances, the products are favored thermodynamically the lower the water content of the solvent, but they are disfavored kinetically. In solvents with less water these equilibria are not rapidly established; indeed, in certain circumstances they become the rate-controlling steps.

In accord with earlier findings, both **A** and **B** react with the substrate. Their respective second-order rate constants are designated k_3 and k_4 , eq 3-4.



The rate law for product buildup, assuming the steady-state approximation, can be derived. Actually, as in this case and in those for catalytic reactions such as those represented by the Michaelis-Menten mechanism, this is really the situation sometimes referred to as "improved" steady-state kinetics.²⁰ The resulting rate law needs to be written in terms of $[\text{Re}]_{\text{T}}$ rather than $[\text{MTO}]$, to allow for varying distributions among the three forms of rhenium with varying concentrations and sometimes with time. With **D** representing Diene and **P** product is

$$\frac{d[P]}{dt} = \frac{k_1 k_3 [Re]_T [H_2O_2] [D] + \frac{k_1 k_2 k_4 [Re]_T [D] [H_2O_2]^2}{k_4 [D] + k_{-2}}}{k_{-1} + k_3 [D] + k_1 [H_2O_2] + \frac{k_1 k_2 [H_2O_2]^2}{k_4 [D] + k_{-2}}} \quad (5)$$

To simplify the treatment implied by the complete equation, conditions were set to attain one or another limiting form. In the one case, the concentration of the diene was chosen to be higher than that of hydrogen peroxide. The actual concentrations were chosen in combination with the rate constants, to make the second numerator term negligible and the second denominator term dominant. With that, eq 5 simplifies to the form

$$\frac{d[P]}{dt} = k_1 [Re]_T [H_2O_2] \quad (6)$$

The reaction of 2,5-dimethyl-2,4-hexadiene provides an example of this limit. With constant concentrations of hydrogen peroxide (4 mM), water (2.2 M) and diene (6 mM), the concentration of MTO was varied, 4–8 mM. The initial rate of reaction, v_i , was evaluated from each experiment. The plot of v_i against $[Re]_T$ at constant $[H_2O_2]$ was linear, as was the plot of v_i against $[H_2O_2]$ at constant $[Re]_T$. To consolidate the presentation of the kinetic data obtained under these conditions, we display in Figure 1 a plot of v_i against the concentration product $[Re]_T \times [H_2O_2]$. The data define an excellent straight line, with a slope $k_1 = 0.484 \pm 0.002 \text{ L mol}^{-1} \text{ s}^{-1}$. This point agrees well with the value one can interpolate from published data.¹⁹ To check this method of data analysis, similar experiments were performed with PhSMe. The initial rate data for this compound was also determined as a function of the two concentrations. The results are also displayed in Figure 1, where it is seen that they are essentially coincident with those for the diene.

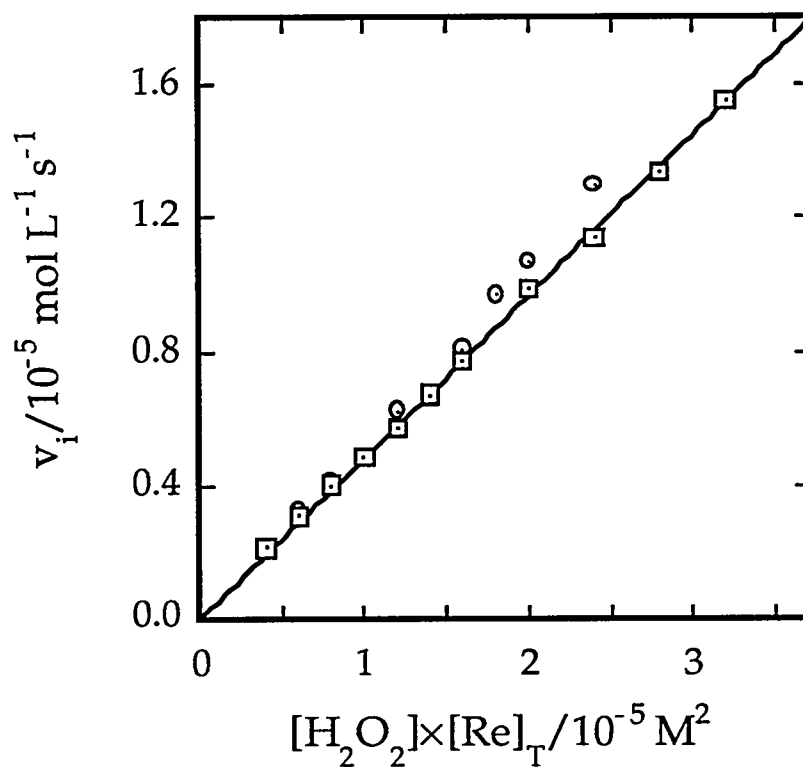


Figure 1. Kinetic data at relatively low concentrations of hydrogen peroxide shown as a plot of the initial rate (v_i) for the oxidation of 2,5-dimethyl-2,4-hexadiene, represented by squares, against the product of two concentrations, $[\text{Re}]_{\text{T}} \times [\text{H}_2\text{O}_2]$. The slope of the line defines k_1 . The coincident data defined by the oxidation of thioanisole is given by the circles.

This aspect of the work was carried no further, however, since kinetic studies carried out under these conditions provide no information other than the already-known rate of interaction of MTO with hydrogen peroxide. Thus other conditions were employed for most of the kinetics experiments.

Data that are more informative as to the oxygen-transfer step of the reaction were obtained when the concentration of the diene, 0.20–20 mM, was taken to be much lower than that of hydrogen peroxide, itself at a much higher concentration, 0.50 M. Again, these experiments were done with $[H_2O]$ maintained at 2.2 M (otherwise the activity water would change significantly with varying $[H_2O_2]$) and variable $[Re]_T$, 0.1–20 mM, or 100 mM on occasion. At these concentration ranges, the limiting form becomes

$$-\frac{d[D]}{dt} = \frac{d[P]}{dt} = k_4[Re]_T[D] \quad (7)$$

Since the catalyst concentration remains constant, the reaction follows pseudo-first-order kinetics. The rate constant so obtained, labeled k_ψ , is expected to be a linear function of $[Re]_T$, but not expected to show other dependences. **Figure 2** confirms the linearity of the variation, with data shown for two dienes, 2,4-hexadiene and cis-piperylene (cis-1,3-pentadiene), each at 4 mM concentration. From the slopes of the lines, the respective values of k_4 are 0.401 ± 0.002 and 0.119 ± 0.005 ; the standard deviations represent the goodness of the fit to the line, and the true precision considering various sources of random error is perhaps $\pm 5\%$. The rate constants so determined for 16 conjugated dienes and 1 nonconjugated analog are presented in **Table 1**.

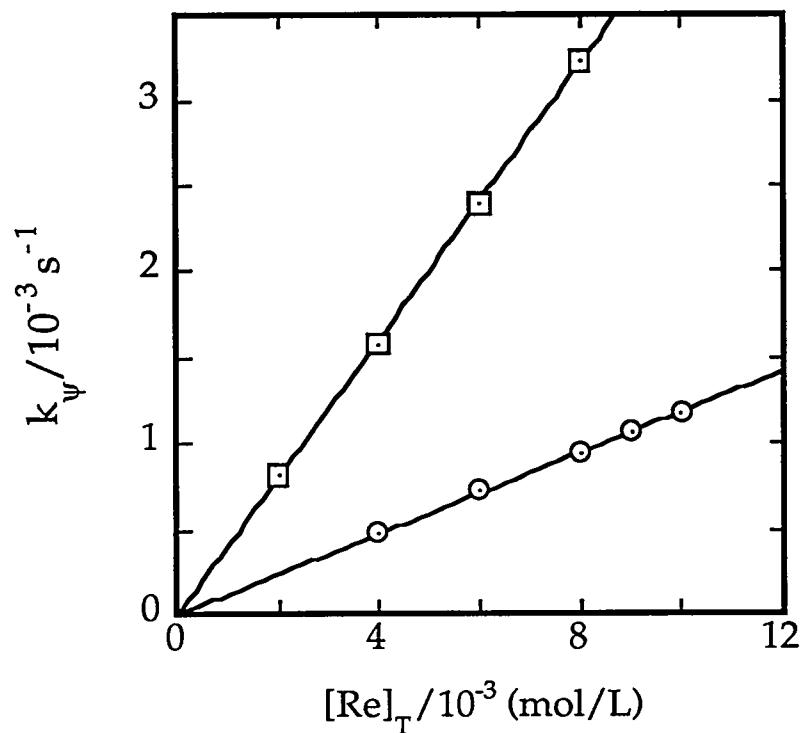


Figure 2. The pseudo-first-order rate constants for the oxidation reactions of 2,4-hexadiene and cis-piperylene (cis-1,3-pentadiene) (each 4 mM) by hydrogen peroxide (0.50 M) in acetonitrile containing 2.2 M water vary linearly with the total rhenium concentration, in accord with eq 7.

Table 1. Rate constants and products for the MTO-catalyzed oxidation of (mostly) conjugated dienes by hydrogen peroxide.

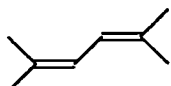
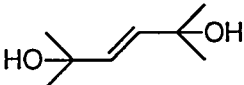
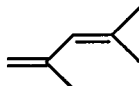
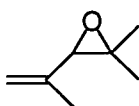
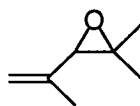
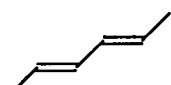
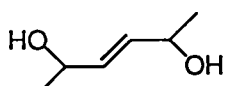
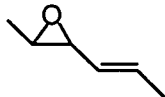
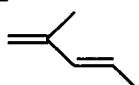
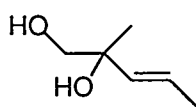
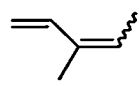
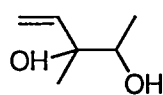
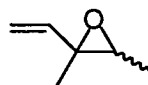
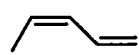


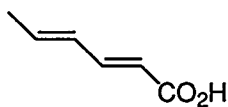
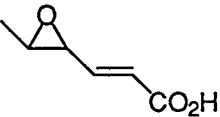

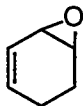
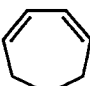
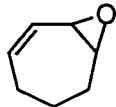
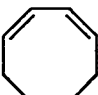
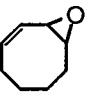
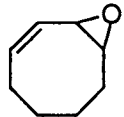
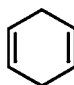
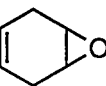
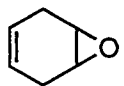
Entry	Diene	k_4 /L mol ⁻¹ s ⁻¹	Product w/ H ₂ O ₂	% Yield ^a	Product with UHP ^b	% Yield ^a
1	2,5-Dimethyl-2,4-hexadiene 	3.92		82		
2	2,4-Dimethyl-1,3-pentadiene 	0.562		45		58
3	2,4-Hexadiene (80% trans-trans) 	0.401		62		79
4	trans-2-Methyl-1,3-pentadiene 	0.324		61		
5	3-Methyl-1,3-pentadiene (cis:trans = 1:1.4) 	0.294		77	 (cis : trans = 1 : 1.4)	91
6	cis-Piperylene (1,3-Pentadiene) 	0.120		72		84

Table 1. (continued)

Entry	Diene	k_4 /L $\text{mol}^{-1} \text{s}^{-1}$	Product w/ H_2O_2	% Yield ^a	Product with UHP ^b	% Yield ^a
7	trans-Piperylene (1,3-Pentadiene) 	0.105		65		70
8	2,3-Dimethyl-1,3-butadiene 	0.0867		69		86
9	Isoprene (2-methyl-1,3-butadiene) 	0.0714		74		88
10	1-Methoxy-1,3-butadiene (cis & trans) 	1.47		67		
11	2,3-Dimethoxy-1,3-butadiene 	1.36		85		
12	trans,trans-2,4-Hexadien-1-ol 	0.297		64		

Table 1. (continued)

Entry	Diene	k_4 /L mol ⁻¹ s ⁻¹	Product w/ H ₂ O ₂	% Yield ^a	Product with UHP ^b	% Yield ^a
13	trans, trans-2,4- Hexadienoic acid 	0.00410		94		
14	1,3- Cyclohexadiene 	1.00	mixture of diols			86
15	1,3- Cycloheptadiene 	0.387	mixture of diols			93
16	cis,cis-1,3- Cyclooctadiene 	0.189		80		96
17	1,4- Cyclohexadiene 	0.102		75		85

^a Based on ¹H NMR peak integrations; ^b UHP = NH₂CONH₂·H₂O₂

Products. We used ^1H NMR, ^{13}C NMR, and GC-MS to identify the reaction products. They are also shown in each case in Table 1, along with the reaction yields. As with the kinetics, the products were studied in the case where hydrogen peroxide was used. Most (but interestingly, not all) of the products were diols; if, however, the products were monitored early in the reaction, largely the epoxides were detected. To no surprise, then, the epoxides are undergoing a ring-opening reaction during the course of the reaction.

In an attempt to minimize diol formation, many of the reactions were carried out with the solid reagent urea hydrogen peroxide (UHP, $\text{H}_2\text{NC(O)NH}_2\cdot\text{H}_2\text{O}_2$) and without any addition of water to the acetonitrile. In these cases, most of the dienes gave only epoxides, Table 1. The UHP reactions are heterogeneous, and thus have no applications for kinetics, but they do provide a useful means of obtaining the desired epoxides.

Epoxide stability to UHP. Certain of the epoxides were tested with UHP and MTO for an extended time. Provided water was absent, the epoxides could be kept for one week without evidence of ring opening. On the other hand, when water (2.2 M) was added to the reaction, diol was formed over several hours. When instead perhenic acid (10 mM), 2-methyl-2-vinyloxirane (0.20 M), and water (2.2 M) were combined, the ring opening reaction finished in several hours. With 2-methyl-3-vinyloxirane, the reaction time was several days.

Discussion

Kinetic model. The reaction sequence, a combination of Scheme 1 and eq 3-4, represents the essence of the mechanism. As shown, both of the peroxorhenium compounds are active catalysts. Under most of the conditions employed here, however, the contribution of A was negligible compared to that

of **B**, and the direct reaction between **B** and the alkene, eq 4, was rate-controlling. The occurrence of this reaction gave rise to **A**, not MTO, and so nearly all of the catalytic cycle involves the re-cycling of **A** to **B** via the step of **Scheme 1** with the rate constant k_2 .

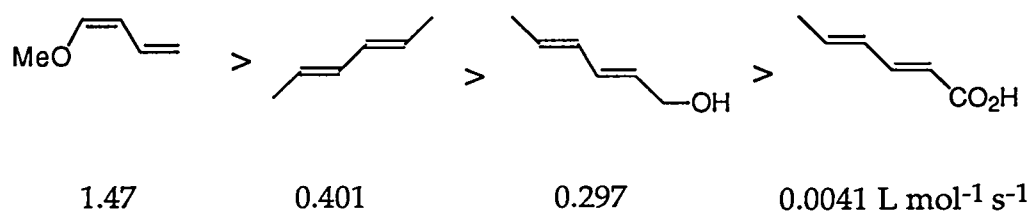
The subsequent step that gives rise to diols is often faster than epoxide formation, but not always. The relative rates of these steps are immaterial in the kinetic analysis, however, since the UV monitoring procedure for the first reaction experiences almost no distortion from the subsequent reaction of the epoxide. As shown in **Table 1**, some of diol formation is accompanied by rearrangement, owing to the relative stability of carbocation intermediates, as will be explained.

Kinetic effects of substituents. Previous data have shown that substituents have a regular effect on the rate, depending on the direction in which they alter the electron density at the double bond: an electron-donating group increases the value of k_4 , whereas an electron-attracting group lowers it.¹⁰ First, let us examine the effect of replacing one or more diene protons by methyl groups. From **Table 1**, we can examine the rate ratios for these substituents. These are the comparisons: hexadienes, Entries 1 and 3, k_4 ratio 9.8; pentadienes, Entries 2–7, ratios 2.5–5.3; butadienes, Entries 6–9, ratios 1.2–1.7. The indicated accelerations are clear.

To express this effect in graphic terms, we display in **Figure 3** a plot of $\log k_4$ against the number of methyl substituents on the nine compounds shown as Entries 1–9. In constructing this plot, the rate constant of the symmetric diene, Entry 1, was divided by 2 to provide a statistical correction. A straight line was drawn through the values, which span two orders of magnitude in rate, with a correlation coefficient 0.992. The linearity of the correlation is not the issue,

however. This graph is simply to show how consistent the effects of electron-donating methyl groups are. This shows how the electron-rich dienes are more rapidly epoxidized by MTO/H₂O₂. It would be of considerable interest to compare quantitatively the extent of correlation with diene epoxidation rate constants with other catalysts. As remarked earlier, systematic studies are lacking in the literature.

Further examples of the effect of electron-donating and electron-attracting substituents can be seen in this series of compounds, the k_4 values for which are shown:



It is interesting to explore the reason behind the diminution of the reactivity of the cyclic conjugated 1,3-dienes with C₆, C₇, and C₈ rings. The ground-state conformations of these compounds have been thoroughly studied.²¹ The degree of conjugation decreases with ring size owing to the conformational preferences of the carbocyclic ring. The parameters for these compounds are given in Table 2, along with values for the non-conjugated compounds 1,4-cyclohexadiene and cyclohexene.

Very clearly, effective conjugation, such as exists in 1,3-cyclohexadiene, exerts a rate-enhancing effect. Compare the much larger rate constant for this compound ($k_4/2 = 0.50 \text{ L mol}^{-1} \text{ s}^{-1}$) with those for two nonconjugated counterparts, 1,4-cyclohexadiene ($k_4/2 = 0.051 \text{ L mol}^{-1} \text{ s}^{-1}$) and cyclohexene ($k_4 = 0.108 \text{ L mol}^{-1} \text{ s}^{-1}$).¹⁰

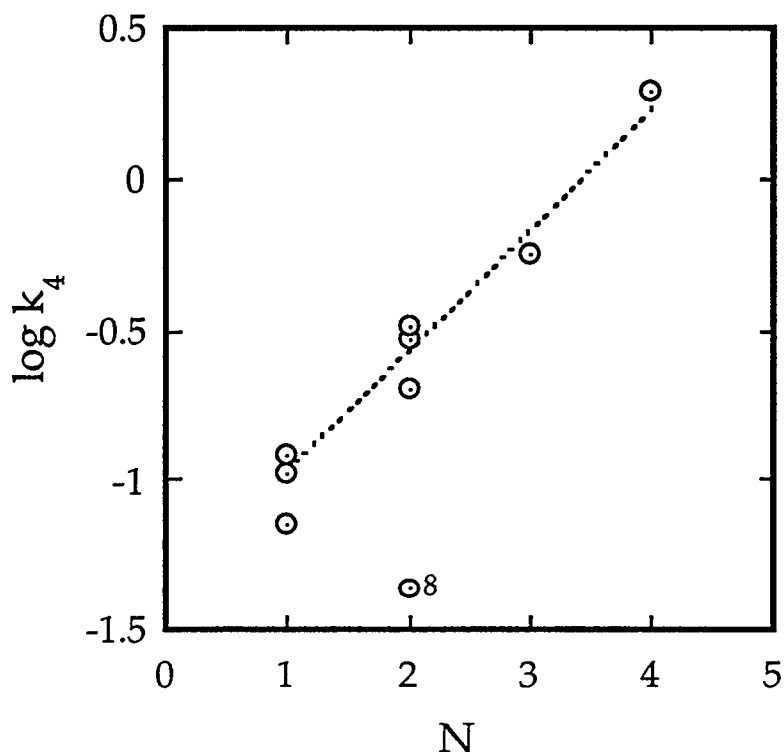
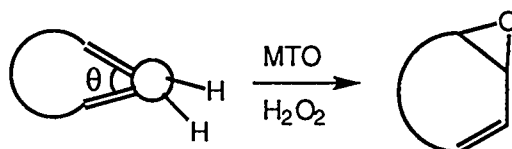


Figure 3. Correlation of the rate constants ($\log k_4$) for the epoxidation of conjugated dienes and **B**, with the number of methyl groups on the diene. Entry 8 from Table 1 is noted, in that it fails in this correlation.

On the other hand, ring size appears to play an important role, with a decrease in rate along the series $C_6 > C_7 > C_8$. This effect can actually be traced to a decline in conjugation. Note that the dihedral angle is wider for 1,3-cycloheptadiene and wider yet for 1,3-cyclo-octadiene; this widening of the dihedral angle lessens the extent of conjugation. The respective rate constants, $k_4/2 = 0.19$ and $0.095 \text{ L mol}^{-1} \text{ s}^{-1}$, are clearly much smaller than for compounds (e.g., 1,3-cyclohexadiene and 2,4-hexadiene) whose structures allow nearly the full extent of conjugation.

Table 2. MTO-Catalyzed Epoxidations of Cyclic Dienes in Comparison with Mono-enes



Diene, Mono-ene	θ	$k_4 / \text{L mol}^{-1} \text{s}^{-1}$
	10°	1.00
	22°	0.387
	55°	0.189
		0.102
		$2k_4 = 0.22$

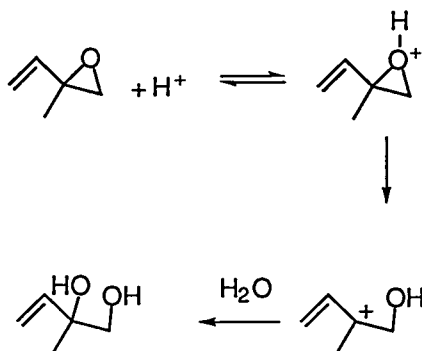
On the other hand, ring size appears to play an important role, with a decrease in rate along the series $\text{C}_6 > \text{C}_7 > \text{C}_8$. This effect can actually be traced to a decline in conjugation. Note that the dihedral angle is wider for 1,3-cycloheptadiene and wider yet for 1,3-cyclo-octadiene; this widening of the dihedral angle lessens the extent of conjugation. The respective rate constants, $k_4/2 = 0.19$ and $0.095 \text{ L mol}^{-1} \text{s}^{-1}$, are clearly much smaller than for compounds (e.g., 1,3-cyclohexadiene and 2,4-hexadiene) whose structures allow nearly the full extent of conjugation.

A further correlation was attempted between the rate constant, statistically corrected by a factor of two for the symmetric dienes, and the energy of the $\pi \rightarrow \pi^*$ transition as determined from the UV spectrum.²² Figure 4 displays a plot of log

(k_4) against energy for all the hydrocarbons, oxygenated compounds being omitted. There is a reasonable correlation, although one entry lies well off the approximate line defined by the others. The deviant point represents Entry 8 in Table 1, the same compound furthest off the line in Figure 3 as well. (We can offer no rationale for it.) This correlation tells us that the chemistry of the epoxidation process is that of an electron-rich double bond nucleophilically attacking the coordinated peroxo ligand in that it correlated with the excitation energy for an electron in that very bond.

Epoxide disappearance. Many of the reactions produce exclusively or primarily vic-diols. The ring-opening reactions that produce this result are well known.²³ Scheme 2 shows the pertinent steps, the most prominent feature being the intervention of a carbocation intermediate. The relative stabilities of the carbocations govern the rate of ring opening. For example, the ring-opening rate of 2-methyl-2-vinyloxirane is much higher than that of 2-methyl-3-vinyloxirane owing the higher stability of the tertiary carbocation intermediate in the rate-controlling step of ring opening. In this way, we can account for the major product being the epoxide from 1,3-pentadiene, but the diol with isoprene (2-methyl-1,3-butadiene), this pair being related in just the way described.

Scheme 2



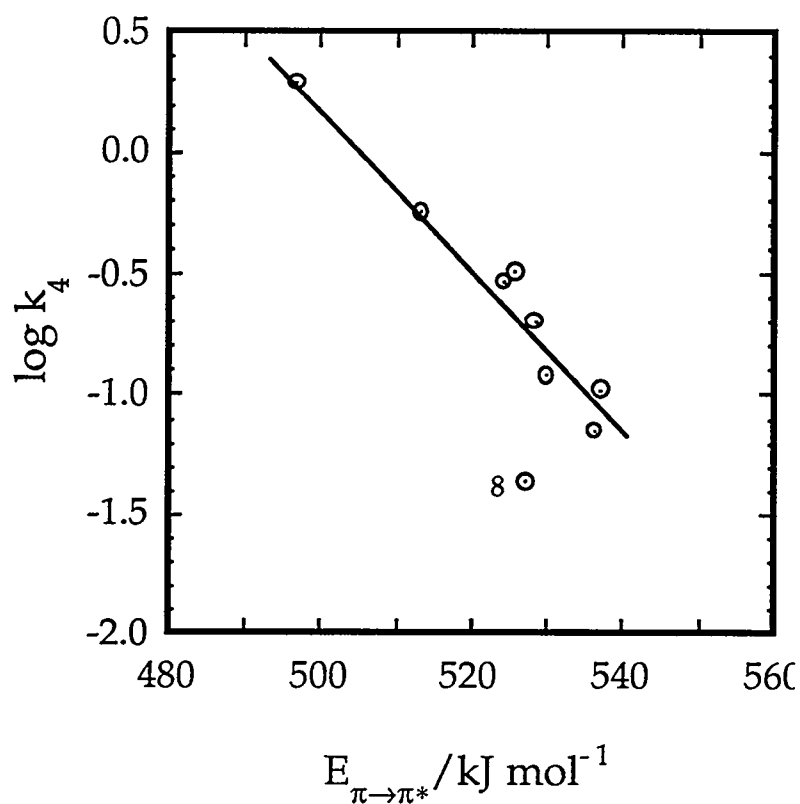
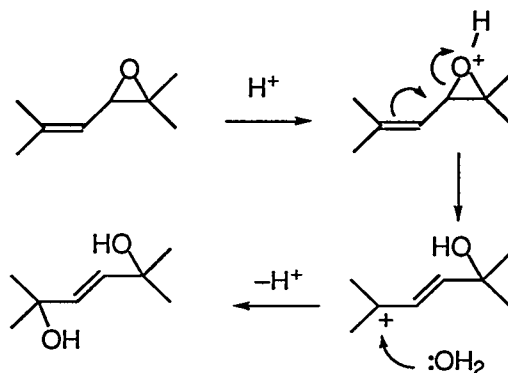


Figure 4. Correlation of the rate constants ($\log k_4$) for the epoxidation of conjugated dienes and **B**, with the energy of the $\pi \rightarrow \pi^*$ UV transition for the conjugated diene. Entry 8 from Table 1 is noted, in that it fails in this correlation.

The enthalpy of formation of the two epoxides obtainable from trans-2-methyl-1,3-pentadiene were calculated by use of the CAChe program.²⁴ The value of ΔH°_f for 2-methyl-2-propenyloxirane, $-35.4 \text{ kJ mol}^{-1}$, is about 21% lower than that for 2-isopropenyl-3-methyloxirane, $-28.3 \text{ kJ mol}^{-1}$. This driving force may provide an additional reason for the formation of the former compound.

Rearrangements leading to 1,4-diols. Note that two reactions, Entries 1 and 3, give rise not to geminal diols but to diols in which the two OH groups are in relative 1 and 4 positions. This change arises because secondary and tertiary carbocations are more stable than the initially-formed primary ones. This is shown in Scheme 3 for the epoxide derived from 2,5-dimethyl-2,4-hexadiene.

Scheme 3



We conclude, therefore, that the MTO-catalyzed epoxidations are controlled in rate by the electron density at the double bond and by the extent of conjugation of the double bonds, most noticeably so when they coexist in a cyclic system. The primarily-produced epoxide is that at the most electron-rich of the double bonds, when there is a difference. Epoxides are obtained when UHP is used instead of hydrogen peroxide, since the activity of water is low, and also when the epoxide undergoes slow a ring-opening reaction, as when the carbocation intermediate is unstable. It seems clear that UHP provides a cleaner route when the epoxides are desired, without sacrifice of reactivity, both being complete in 2-3 hours under the conditions described.

Acknowledgment. This research was supported by the U. S. Department of Energy, Office of Basic Energy Sciences, Division of Chemical Sciences under contract W-7405-Eng-82.

Supporting Information Available: The ^1H -NMR ^{13}C -NMR and mass spectral data for the products is contained in many libraries on microfiche, immediately following this article in the microfilm version of the journal, can be ordered from the ACS, and can be downloaded from the Internet; see any current masthead page for ordering information and Internet access instructions.

Supporting Information for the paper

Kinetics and Mechanism of the Dihydroxylation and Epoxidation of Conjugated Dienes with Hydrogen Peroxide Catalyzed by Methylrhenium Trioxide

Haisong Tan and James H. Espenson

NMR (in CD_3CN) and MS data

2,5-dimethyl-hex-3-ene-2,5-diol (1a) ^1H NMR, δ/ppm 5.69(s, 2H), 1.21(s, 12H); ^{13}C NMR, δ/ppm 133.63, 81.43, 23.31.

3,4-epoxy-2,4-dimethyl-pent-1-ene (2a) ^1H NMR, δ/ppm 4.91-4.93(m, 1H), 4.76-4.78(m, 1H), 3.13(s, 1H), 1.73(m, 3H), 1.32(s, 3H), 1.31(s, 3H); ^{13}C NMR, δ/ppm 140.17, 110.11, 64.96, 59.58, 24.85, 18.69, 16.28. MS(EI): 112(M^+ , 10%), 97(100%), 83(25%), 69(33%).

Hex-3-ene-2,5-diol (3a) ^1H NMR, δ/ppm 5.62(m, 2H), 4.18(m, 2H), 1.18(d, 6H); ^{13}C NMR, δ/ppm 132.95, 132.83, 67.31, 67.20, 21.99, 21.93.

4,5-epoxy-hex-2-ene (3b) ^1H NMR, δ/ppm 5.90-6.00(m, 1H), 5.18-5.21(m, 1H), 3.00-3.03(dd, $J=8.4, 2.0$ Hz, 1H), 2.85-2.87(m, 1H), 1.69-1.71(dd, $J=6.4, 1.6$ Hz, 3H), 1.24-

1.26(d, $J=4.2$ Hz, 3H); ^{13}C NMR, δ/ppm 130.70, 128.67, 58.78, 55.35, 16.71, 16.43.; MS(EI): 99[(M+H) $^+$, 39%], 83(100%), 65(16%).

2-methyl-pent-3-ene-1,2-diol (4a) ^1H NMR, δ/ppm 5.66-5.71(m, 1H), 5.48-5.54(dd, $J=15.6, 1.5$ Hz, 1H), 3.31-3.32(d, $J=3.6$ Hz, 2H), 1.66-1.69(dd, $J=6.9, 1.5$ Hz, 3H), 1.16(s, 3H); ^{13}C NMR, δ/ppm 139.08, 127.72, 72.40, 69.14, 23.12, 16.76.

3-methyl-pent-4-ene-2,3-diol (5a) ^1H NMR, δ/ppm 5.89-5.99(m, 1H), 5.22-5.34(m, 1H), 5.12-5.16(m, 1H), 3.59-3.63(q, 1H), 1.18-1.21(d, $J=8.8$, 3H), 1.07-1.09(d, $J=6.8$ Hz, 3H); ^{13}C NMR, δ/ppm 141.87, 113.15, 75.41, 73.02, 22.51, 16.41.

3,4-epoxy-3-methylpentene (5b) Cis: ^1H NMR, δ/ppm 5.76-5.86(dd, $J=17.7, 10.8$ Hz, 1H), 5.28-5.30(m, 1H), 5.23-5.25(m, 1H), 2.96-3.02(q, 1H), 1.34(s, 3H), 1.15-1.18(d, $J=5.4$ Hz, 3H); ^{13}C NMR, δ/ppm 136.19, 116.79, 60.67, 59.61, 13.58, 12.70. **Trans:** ^1H NMR, δ/ppm 5.60-5.70(dd, $J=17.7, 10.8$ Hz, 1H), 5.25-5.32(dd, $J=17.7, 1.2$ Hz, 1H), 5.11-5.16(dd, $J=10.8, 1.2$ Hz, 1H), 2.86-2.91(q, 1H), 1.32(s, 3H), 1.24-1.27(d, $J=5.4$ Hz, 3H); ^{13}C NMR, δ/ppm 141.00, 114.76, 60.17, 58.65, 20.17, 12.90.

Pent-4-ene-2,3-diol (6a) ^1H NMR, δ/ppm 5.80-5.89(m, 1H), 5.25-5.30(d, $J=17.2$, 1H), 5.14-5.17(d, $J=10.4$ Hz, 1H), 3.76-3.80(m, 1H), 3.51-3.58(m, 1H), 1.06-1.08(d, $J=6.4$ Hz, 3H); ^{13}C NMR, δ/ppm 137.70, 115.53, 76.64, 69.72, 17.64.

Cis-3,4-epoxy-pent-1-ene (6b) ^1H NMR, δ/ppm 5.69-5.81(m, 1H), 5.43-5.51(dd, $J=17.1, 1.8$ Hz, 1H), 5.33-5.38(dd, $J=10.5, 1.8$ Hz, 1H), 3.34-3.38(dd, $J=7.2, 4.5$ Hz, 1H), 3.15-3.19(m, 1H), 1.21-1.24(d, $J=5.7$ Hz, 3H); ^{13}C NMR, δ/ppm 132.97, 119.83, 56.70, 53.91, 12.42.

Trans-3,4-epoxy-pent-1-ene (7b) ^1H NMR, δ/ppm 5.52-5.60(m, 1H), 5.41-5.49(dd, $J=17.1, 2.1$ Hz, 1H), 5.22-5.26(dd, $J=9.9, 2.1$ Hz, 1H), 3.04-3.08(dd, $J=7.2, 2.1$ Hz, 1H),

2.87-2.90(m, 1H), 1.26-1.28(d, $J=5.1$ Hz, 3H); ^{13}C NMR(CD_3CN), δ/ppm 136.00, 118.05, 59.78, 55.60, 16.35.

2,3-dimethyl-but-3-ene-1,2-diol (8a) ^1H NMR, δ/ppm 5.00(br, 1H), 4.86-4.87(m, 1H), 3.49-3.52(d, $J=9.0$ Hz, 1H), 3.36-3.40(d, $J=9.0$ Hz, 1H), 1.74(s, 3H), 1.20(s, 3H); ^{13}C NMR, δ/ppm 148.79, 109.88, 75.03, 67.64, 22.64, 18.39; MS(NH_3/CI), 134.0($\text{M}+\text{NH}_4^+$, 100%), 116.1(M^+ , 14%).

3,4-epoxy-2,3-dimethylbutene (8b) ^1H NMR, δ/ppm 5.03(br, 1H), 4.92-4.93(m, 1H), 2.70-2.72(d, $J=5.4$ Hz, 1H), 2.65-2.67(d, $J=3.4$ Hz, 1H), 1.68(s, 3H), 1.39(s, 3H); ^{13}C NMR, δ/ppm 145.01, 111.48, 57.17, 53.12, 19.48, 17.28.

2-methyl-but-3-ene-1,2-diol (9a) ^1H NMR, δ/ppm 5.88-5.95(dd, $J=17.6, 10.8$, 1H), 5.23-5.28(dd, $J=17.6, 1.2$ Hz, 1H), 5.10-5.14(dd, $J=10.8, 1.2$ Hz, 1H), 3.41(s, 1H), 3.40(s, 1H), 1.21(s, 3H); ^{13}C NMR, δ/ppm 141.85, 112.91, 73.31, 68.62, 22.64.

3,4-epoxy-3-methylbutene (9b) ^1H NMR(CD_3CN), δ/ppm 5.58-5.68(dd, $J=17.4, 10.8$, 1H), 5.31-5.38(dd, $J=17.4, 1.2$ Hz, 1H), 5.18-5.23(dd, $J=10.8, 1.2$ Hz, 1H), 2.75-2.78(d, $J=5.4$ Hz, 1H), 2.66-2.69(d, $J=5.4$, 1H), 1.39(s, 3H); ^{13}C NMR, δ/ppm 139.53, 115.96, 54.92, 54.60, 17.77.

2-hydroxy-but-3-enal (10a) ^1H NMR, δ/ppm 9.53-9.56(d, $J=8.0$ Hz, 1H), 5.83-5.96(m, 1H), 5.28-5.36(dd, $J=17.2, 1.6$ Hz, 1H), 5.17-5.22(dd, $J=10.4, 1.6$ Hz, 1H), 4.04-4.10(m, 1H); ^{13}C NMR, δ/ppm 194.50, 135.96, 101.71, 71.70.; MS(EI): 86(M^+ , 2%), 57(100%).

3-methoxy-1-hydroxy-but-3-ene-2-one (11a) ^1H NMR, δ/ppm 5.20-5.22(d, $J=2.8$ Hz, 1H), 4.66-4.67(d, $J=2.8$ Hz, 1H), 4.54(s, 2H), 3.63(s, 3H); ^{13}C NMR, δ/ppm 196.26, 156.59, 91.04, 64.93, 54.80.; MS(EI): 116(M^+ , 35%), 98(10%), 86(57%), 57(100%) ; High Resolution Mass: theoretical: 116.04734; measured: 116.04741

Hex-2-ene-1,4,5-triol (12a) ^1H NMR, δ/ppm 5.72-5.80(dd, $J=15.6, 5.7$ Hz, 1H), 5.55-5.64(dd, $J=15.6, 6.6$ Hz, 1H), 4.07-4.28(m, 2H), 3.41-3.51(m, 2H), 1.18-1.21(d, $J=6.6$ Hz, 3H); ^{13}C NMR, δ/ppm 135.60, 128.09, 71.64, 67.26, 65.25, 21.91. MS(CI/ NH_3): 150($\text{M}+\text{NH}_4^+$, 100%), 132(M^+ , 47%).

3-(3-methyl-oxiranyl)-acrylic acid (13b) ^1H NMR, δ/ppm 6.61-6.70(dd, $J=15.9, 7.5$ Hz, 1H), 6.13-6.19(d, $J=15.9$ Hz, 1H), 3.33-3.37(dd, $J=7.2, 1.8$ Hz, 1H), 3.08-3.11(m, 1H), 1.33-1.36(d, $J=5.4$ Hz, 3H); ^{13}C NMR, δ/ppm 167.90, 145.42, 123.28, 57.57, 57.05, 16.20.

3,4-epoxy-cyclohexene (14b) ^1H NMR, δ/ppm 5.87-5.98(m, 2H), 3.44-3.46(m, 1H), 3.16-3.19(m, 1H), 2.14-2.20(m, 1H), 1.94-1.98(m, 2H), 1.52-1.61(m, 1H); ^{13}C NMR, δ/ppm 132.46, 122.93, 54.31, 46.18, 20.18, 20.00; MS(EI): 97[($\text{M}+\text{H}$) $^+$, 79%], 79(100%), 67(60%).

3,4-epoxy-cycloheptene (15b) ^1H NMR, δ/ppm 5.87-5.92(m, 1H), 5.73-5.78(m, 1H), 3.36-3.38(m, 1H), 3.15-3.17(m, 1H), 2.14-2.22(m, 2H), 1.92-2.03(m, 2H), 1.51-1.57(m, 2H); ^{13}C NMR, δ/ppm 137.93, 123.56, 59.91, 52.70, 30.73, 29.09; MS(EI): 111[($\text{M}+\text{H}$) $^+$, 45%], 93(87%), 81(100%), 63(22%).

3,4-epoxy-cyclooctene (16b) ^1H NMR, δ/ppm 5.72-5.81(m, 1H), 5.50-5.55(m, 1H), 3.37-3.40(m, 1H), 3.04-3.08(m, 1H), 2.25-2.35(m, 1H), 2.00-2.08(m, 2H), 1.70-1.80(m, 1H), 1.58-1.67(m, 2H), 1.27-1.48(m, 2H); ^{13}C NMR, δ/ppm 133.96, 122.21, 57.25, 52.85, 28.32, 26.80, 24.96, 24.49; MS(EI): 124(M^+ , 1.8%), 109(9.2%), 95(72%), 81(100%), 67(60%); MS(CI/ NH_3): 142($\text{M}+\text{NH}_4^+$, 72%), 124(M^+ , 89%), 107(100%).

4,5-epoxy-cyclohexene (17b) ^1H NMR, δ/ppm 5.40-5.41(m, 2H), 3.20-3.22(m, 2H), 2.43-2.44(m, 4H); ^{13}C NMR, δ/ppm 121.19, 50.55, 24.21.

References

- (1) Simándi, L. I. *Catalytic Activation of Dioxygen by Metal Complexes*; Kluwer Academic Publishers: Dordrecht, 1992, p 109.
- (2) Sheldon, R. A.; Kochi, J. K. *Metal-Catalyzed Oxidations of Organic Compounds*; Academic Press: New York, 1981, p 275.
- (3) Goor, G. *Catalytic Oxidations with Hydrogen Peroxide as Oxidant*; Strukul, G., Ed.; in Kluwer Academic Publishers: Dordrecht, 1992, p 25.
- (4) Sheldon, R. A. *Topics in Chemistry* **1993**, *164*, 23.
- (5) Clerici, M. G.; Ingallina, P. *Clean Oxidation Technologies: New Prospects in the Epoxidation of Olefins*; in *Green Chemistry*; American Chemical Society: Washington, DC, 1996, Chapter 5.
- (6) Sheldon, R. A. *Synthesis of Oxiranes*; Cornelis, B. and Herrmann, W. A., Ed.; in *Applied Homogeneous Catalysis with Organometallic Compounds*; VCH: Weinheim, 1996; Vol. 1, p 411.
- (7) Herrmann, W. A.; Fischer, R. W.; Scherer, W.; Rauch, M. U. *Angew. Chem., Int. Ed. Engl.* **1993**, *32*, 1157.
- (8) Herrmann, W. A.; Fischer, R. W.; Rauch, M. U.; Scherer, W. *J. Mol. Catal.* **1994**, *86*, 243.
- (9) Al-Ajlouni, A.; Espenson, J. H. *J. Am. Chem. Soc.* **1995**, *117*, 9243.
- (10) Al-Ajlouni, A.; Espenson, J. H. *J. Org. Chem.* **1996**, *61*, 3969.
- (11) Rudolph, J.; Reddy, K. L.; Chiang, J. P.; Sharpless, K. B. *J. Am. Chem. Soc.* **1997**, *119*, 6189.
- (12) Sheng, M. N.; Zajacek, J. G. *J. Org. Chem.* **1970**, *35*, 1839.
- (13) Suslick, K. S.; Cook, B. R. *J. Chem. Soc., Chem. Commun.* **1987**, 200.
- (14) Birgit Schiott, D. T.; Jorgensen, K. A. *J. Chem. Soc., Chem. Commun.* **1992**, 1072.

- (15) Xu, D.; Crispino, G. A.; Sharpless, K. B. *J. Am. Chem. Soc.* **1992**, *114*, 7570.
- (16) Chang, S.; Lee, N. H.; Jacobsen, E. N. *J. Org. Chem.* **1993**, *58*, 6939.
- (17) Espenson, J. H.; Abu-Omar, M. M. *Adv. Chem. Ser.* **1997**, *253*, 99.
- (18) Hansen, P. J.; Espenson, J. H. *Inorganic Chemistry* **1995**, *34*, 5839.
- (19) Wang, W.; Espenson, J. H. *Inorg. Chem.* **1997**, in press.
- (20) Espenson, J. H. *Chemical Kinetics and Reaction Mechanisms*, 2d Ed.; 2 ed.; McGraw-Hill, Inc.: New York, 1995.
- (21) Collman, J. P.; Brauman, J. I.; Meunier, B.; Hayashi, T.; Kodadek, T.; Raybuck, S. A. *J. Am. Chem. Soc.* **1983**, *107*, 2000.
- (22) We are grateful to Professor R. J. Angelici for the idea of trying this correlation.
- (23) Long, F. A.; Pritchard, J. G. *J. Am. Chem. Soc.* **1956**, *78*, 2663.
- (24) Stewart, J. J. *J. Comp. Chem.* **1989**, *10*, 221.

CHAPTER III

REGIOSELECTIVE OXIDATIVE CYCLIZATION OF HYDROXYALKENES TO
TETRAHYDROFURANS CATALYZED BY METHYLTRIOXORHENIUM

A paper submitted to *Journal of Molecular Catalysis*

Haisong Tan and James H. Espenson

Abstract

The oxidation of 5-hydroxyalkenes by hydrogen peroxide, when catalyzed by MTO, leads to functionalized tetrahydrofurans. In these cases no tetrahydropyran was formed. The results show that the first reaction between the substrate and a peroxorhenium species formed from, and in equilibrium with, MTO and peroxide, yields an epoxide. This intermediate was not detected, however, because cyclization occurred so rapidly. 6-Hydroxyalkenes were similarly but more slowly converted to tetrahydropyran alcohols. A 4-hydroxyalkene was epoxidized but not cyclized.

Keywords: Catalysis; Rhenium; Hydroxyalkene; Peroxide; Oxidation

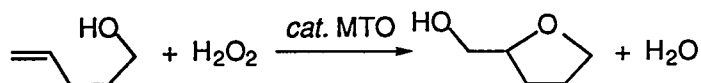
1. Introduction

A number of natural products, such as polyether antibiotics, contain tetrahydrofuran rings [1]. Certain methods have been developed in recent years to synthesize these heterocycles. Among them, chromium [2-5], rhenium [6-8], and thallium [9, 10] oxo reagents are known to induce the oxidative cyclization of monoalkenes, when tethered to a bishomoallylic alcohol. Chromium(VI)-induced cis-oxidative cyclizations of hydroxyalkenes are limited to tertiary alcohols [2-5]. Oxidative cyclization mediated by dirhenium heptoxide produces

predominantly trans-tetrahydrofurfuryl alcohols and is compatible with primary and secondary hydroxyalkenes [6-8]. Thallium acetate, nitrate, and trifluoroacetate induce cyclization of alkenols to tetrahydrofurans [9, 10]. These catalysts, which include Re_2O_7 , have also been used for the oxidative polycyclization of hydroxypolyenes [11-16]. Most of these studies have been directed towards the stereoselective synthesis of substituted tetrahydrofurans. The metal reagents must be taken in relatively high amount (1–3 eq relative to substrate) and the yields are only 50–70%. Peroxy acids can also be used to induce this kind of reaction, but without stereoselectivity [17]. Since methyltrioxorhenium (CH_3ReO_3 , abbreviated as MTO) has proven ability to catalyze peroxide oxidations [18-20], we decided to attempt its use in the case at hand. Our goal was to produce THF derivatives by catalytic oxidation, such that there would be a remaining functional group, in this case CH_2OH , permitting further derivatization. We have attained that goal, and have developed a procedure for that transformation that proceeds with one experimental manipulation. When this work was in progress, we noted a reference to the use of MTO and hydrogen peroxide for the oxidative cyclization of 4-penten-1-ol to tetrahydrofurfuryl alcohol with MTO/ H_2O_2 , with 3-cyanopyridine added to stabilize the catalyst [18].

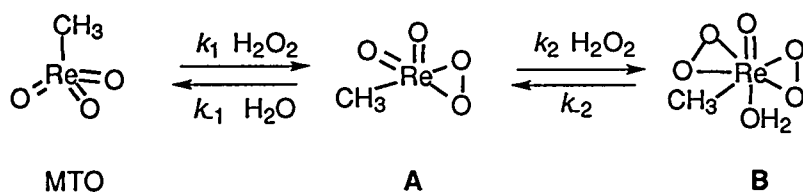
2. Results and Interpretation

Catalysis by MTO. We have found that MTO functions as an efficient catalyst with hydrogen peroxide to make tetrahydrofurfuryl alcohols from 5-hydroxyalkenes. This method achieves nearly complete regioselectivity and has been used successfully with primary, secondary and tertiary 5-hydroxyalkenes. The net reaction for the parent 4-penten-1-ol is given by:



This reaction occurs to 100% conversion with 98% selectivity for this product under mild conditions. The first seven entries in Table 1 illustrate the same reaction for compounds with a methyl substituent on either position of the olefin or on the carbon bearing the OH group. These are reactions in which only a single geometric isomer of the product is possible. They went to 100% conversion, yielding the tetrahydrofurans with >95% selectivity. These examples show that an alkyl group on carbon does not alter the course of the reaction.

As to the mechanism followed, MTO-catalyzed reactions of hydrogen peroxide are well known [19-22]. The active forms of MTO are its monoperoxo and diperoxo complexes, designated **A** and **B**, respectively [19]:



MTO-catalyzed reactions, epoxidations in particular, have been thoroughly documented [23-27]. Comparison of these results to the earlier data allows us to conclude that epoxidation occurs in the initial stage between **A** and/or **B**, depending on the concentration of hydrogen peroxide. Indeed, that step is rate-controlling, because no epoxide buildup was evident in the ^1H spectra taken throughout the reaction. This shows that the epoxide was consumed in a faster step. In support of that, we note that the less substituted alkenes are the least reactive, as judged by the required reaction times in Table 1. The same trend has been independently determined for epoxidations [23-25].

Table 1. Products ^a of the MTO-catalyzed oxidative cyclization of hydroxyalkenes

Entry	Reactant	Product ^b	Yield	Rxn
			(%)	time/h
1			98	6
2			95	3
3			96	6
4			95	6
5			97	6
6			98	2
7			95	2

^a A single enantiomer is shown for entry 7; a d,l-mixture was formed;

^b Products 1, 8 and 11 are commercially available. The following compounds are known compounds; their NMR and mass spectra matched the data given in the references cited: Entry 2, [29] 3, [30] 5, [31] 6, [32] 9, [30] 10, [33] 12, [34, 35] 13, [36, 17] 14, [37, 38] 15, [39-42] 16, [43] 18, [13] 19, [13] 20, [44, 45] and 21. [46]

Table 1. (continued)

Entry	Reactant	Product ^b	Yield (%)	Rxn time/h
8			82 ^c	10
9			97	5
10			93	2
11			90	2

^c The balance is the triol.

This reactivity order simply reflects the established trend that the more alkyl substituents on a double bond, the higher the rate; terminal alkenes that lack a methyl group on the double bond are thus the least reactive.

Another experiment was done in acetonitrile with urea-hydrogen peroxide instead of 30% aqueous hydrogen peroxide [25]. 5-Hexen-1-ol could be oxidized to 5,6-epoxy-1-hexanol in 12 h. Then 0.20 M perchloric acid was added and tetrahydropyran-2-methanol was isolated in 92% yield. For 4-penten-1-ol, however, the ring-closing reaction was much faster and the only product with urea-hydrogen peroxide was tetrahydrofurfuryl alcohol.

Ring Formation. Intramolecular nucleophilic substitutions occur in a kinetic order depending on the size of the resulting ring: 5 >> 6 > 3 > 7 > 8 [28],

and the relative rates for forming 5- and 6-membered rings could differ by 10^3 . In accord with these trends, the present set of cyclization reactions shows excellent regioselectivity for the formation of a 5-membered ring (Table 1), although the reactions could conceivably have produced 6-membered rings (in eq 1, for example, 2-hydroxy-oxacyclohexane might instead have been formed). Thus the ring preference here is again $5 \gg 6$. Related to this are the homologous systems, Entries 8 and 9, which are 6-hydroxyalkenes. In these cases the products, which are tetrahydropyran alcohols, do have 6-membered rings. Entry 10 might have closed to a 7-membered ring, but this is so disfavored that only the triol was obtained. When a 4-hydroxyalkene (Entry 11) was used, no oxidative cyclization occurred, and a triol resulted here as well. These triols are simply the product of the acid-catalyzed ring opening of epoxy alcohols.

Isomers. No selectivity was found for the production of cis- vs. trans-geometric isomers (Table 2). When an alkyl group is bound to a carbon atom that becomes part of the ring, then trans and cis isomers are formed. These two are usually produced in comparable yield; such cases are not likely to be useful in synthesis.

Appropriately constituted hydroxydienes (Entries 18, 19) undergo ring formation twice, producing a bistetrahydrofuranyl alcohol. These two examples differ from one another only as regards the geometric isomers of the starting material at the central double bond; they gave geometric isomers of the products. Nonconjugated dienes (Entries 20, 21) differ from conjugated dienes [25], in that only one double bond could be oxidized. The nonconjugated dienes were oxidized very slowly in CHCl_3 . When the solvent was changed to CH_3CN , however, both double bonds were oxidized leading to the hydroxy tetrahydrofuran.

Table 2. Isomeric products of the MTO-catalyzed oxidative cyclization of alkyl-substituted hydroxyalkenes

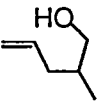
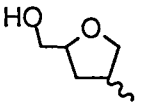
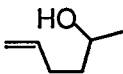

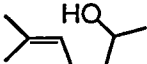
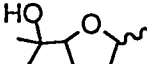
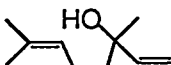
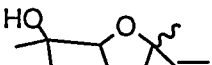

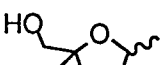
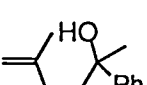
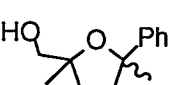
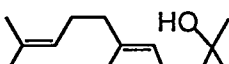
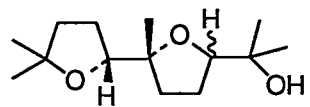
Entry	Reactant	Product (cis:trans)	Yield(%)	Rxn time/h
12		 (0.85 : 1.0)	96	6
13		 (0.82 : 1.0)	95	6
14		 (1.6 : 1.0)	92	1
15		 (0.86 : 1.0)	92	1
16		 (1.0:1.4)	97	2
17		 (1.0 : 1.0)	94	1
18		 (0.81 : 1.0)	91	2

Table 2. (continued)

Entry	Reactant	Product (cis:trans)	Yield(%)	Rxn time/h
19		 (1.3 : 1.0)	90	2
20 ^d		 (1.0 : 1.0)	72	12
21 ^d		 (1.1 : 1.0)	70	12

^d The reaction was carried out in CH₃CN, and the by-products were diol and tetraol.

3. Experimental section

The general procedure employed a scale of 0.4–4 mmol of the hydroxyalkene, allowing the product to be isolated in pure form, under neutral conditions at room temperature using readily-available 30% hydrogen peroxide. The general procedure is this: to 20 μ mol MTO and 0.5–1 mmol H₂O₂ in 1.0 mL chloroform was added 0.4 mmol substrate. Comparable results were obtained at a scale ten times greater, with 100 μ mol MTO; the level of MTO can be lowered further at the cost of a longer reaction time. The heterogeneous mixture was stirred at room temperature for the necessary reaction time. At the completion of the reaction, Na₂CO₃ was added to decompose MTO. The product was extracted

with ether and washed with a small amount of water. To shorten the reaction time, the heterogeneous mixture of 4-penten-1-ol was stirred at 40 °C for an hour. The reaction was finished with same yield shown in Table 1.

The stereochemistry was verified from the ^1H NOE spectra, and the cis:trans ratio determined by integration of the NMR and GC. The products are mostly known compounds, the identities of which were confirmed by matching NMR and mass spectrometric data. The spectroscopic data are summarized in Supporting Information. Three compounds were new: Entries 4, 7, and 17. Their high resolution mass spectra were used for identification purposes; in every case there was an exact match of molecular weights.

Acknowledgment. This research was supported by the U. S. Department of Energy, Office of Basic Energy Sciences, Division of Chemical Sciences under contract W-7405-Eng-82.

Supporting Information

Spectroscopic data for the products: NMR chemical shifts (in CDCl_3) and parent masses

Tetrahydrofurfuryl alcohol (1): ^1H NMR(δ /ppm): 4.01-4.03(m, 1H), 3.78-3.88(m, 2H), 3.63-3.68(m, 1H), 3.48-3.52(m, 1H), 1.89-1.95(m, 3H); 1.62-1.69(m, 1H); ^{13}C NMR(δ /ppm): 79.55, 68.28, 64.88, 27.14, 26.01.

1-tetrahydrofuran-2-yl-ethanol (2): ^1H NMR(δ /ppm): 3.95-3.97(m, 1H), 3.86-3.91(m, 1H), 3.75-3.81(m, 2H), 1.79-1.92(m, 4H), 1.13-1.15(d, $J=6.4\text{Hz}$, 3H); ^{13}C NMR(δ /ppm): 83.06, 68.66, 68.01, 26.06, 24.60, 18.27; MS(EI, 70ev) m/z : 116(M^+ , 3%), 99(100%).

(5,5-dimethyl-tetrahydrofuran-2-yl) methanol (3): ^1H NMR(δ /ppm): 4.06-4.09(m, 1H), 3.62-3.66(m, 1H), 3.44-3.49(m, 1H), 1.93-1.96(m, 1H), 1.70-1.78(m, 3H), 1.25(s,

3H), 1.23(s, 3H); ^{13}C NMR(δ /ppm): 81.67, 79.06, 65.41, 38.60, 29.02, 27.97, 27.78; MS(EI) m/z: 130(M^+ , 52%), 113(12%), 99(20%), 95(100%).

(4,4-dimethyl-tetrahydrofuran-2-yl) methanol (4): ^1H NMR(δ /ppm): 4.15-4.19(m, 1H), 3.63-3.69(m, 1H), 3.48-3.54(m, 3H), 1.57-1.73(m, 1H), 1.44-1.52(m, 1H), 1.11(s, 3H), 1.10(s, 3H); ^{13}C NMR(δ /ppm): 80.04, 79.85, 65.09, 41.94, 39.71, 26.44, 26.06; MS(EI) m/z: 130(M^+ , 98%), 113(62%), 99(40%), 95(100%). HRMS calcd for $\text{C}_7\text{H}_{14}\text{O}_2$ 130.09937, found 130.09937.

(3,3-dimethyl-tetrahydrofuran-2-yl) methanol (5): ^1H NMR(δ /ppm): 3.86-3.93(m, 2H), 3.54-3.61(m, 3H), 1.74-1.80(m, 2H), 1.10(s, 3H), 0.95(s, 3H); ^{13}C NMR(δ /ppm): 87.27, 66.02, 62.63, 41.29, 39.89, 26.34, 21.62; MS(EI) m/z: 130(M^+ , 63%), 113(100%), 99(60%), 95(48%).

(2-methyl-tetrahydrofuran-2-yl) methanol (6): ^1H NMR(δ /ppm): 3.82-3.90(m, 2H), 3.45-3.46(m, 2H), 1.88-1.99(m, 3H), 1.63-1.66(m, 1H), 1.20(s, 3H); ^{13}C NMR(δ /ppm): 83.06, 68.49, 68.06, 33.49, 26.44, 23.29; MS(EI) m/z: 116(M^+ , 4%), 99(100%), 85(28%).

6-hydroxy-hexahydro-cyclopenta**furan(7):** ^1H NMR(δ /ppm): 4.15-4.18(m, 2H), 3.66-3.81(m, 2H), 2.75-2.89(m, 1H), 1.40-2.17(m, 6H); ^{13}C NMR(δ /ppm): 90.85, 77.74, 68.57, 41.21, 34.01, 32.50, 29.81; MS(EI) m/z: 128(M^+ , 23%), 111(15%), 83(100%). HRMS calcd for $\text{C}_7\text{H}_{12}\text{O}_2$ ($\text{M}-\text{CH}_3$) $^+$ 128.08373, found 128.08367.

Tetrahydropyran-2-methanol (8): ^1H NMR(δ /ppm): 3.99-4.03(m, 1H), 3.41-3.58(m, 4H), 1.85-1.87(m, 1H), 1.31-1.57(m, 5H); ^{13}C NMR(δ /ppm): 78.24, 68.33, 66.31, 27.42, 26.01, 22.94.

1-(tetrahydro-pyran-2-yl)-propan-1-ol (9): ^1H NMR(δ /ppm): 3.99-4.04(m, 1H), 3.40-3.46(m, 1H), 3.31-3.34(m, 1H), 3.11-3.16(m, 1H), 1.84-1.88(m, 1H), 1.32-1.58(m, 7H), 0.96-1.00(t, $J=7.2\text{Hz}$, 3H); ^{13}C NMR(δ /ppm): 80.52, 75.55, 68.46, 27.66, 26.00, 25.39, 23.08, 9.80. MS(EI) m/z: 144(M^+ , 5%), 127(72%), 85(100%).

3,7-dimethyl-octane-1,6,7-triol (10): ^1H NMR(δ /ppm): 3.67-3.78(m, 2H), 3.29-3.41(m, 1H), 1.00-1.90(m, 7H), 1.20(s, 3H), 1.15(s, 3H), 0.90-0.93(d, $J=4.2\text{Hz}$, 3H). ^{13}C NMR(δ /ppm): 79.03, 78.11, 73.27, 60.64, 60.57, 39.72, 39.41, 33.89, 33.19, 29.70, 29.17, 28.58, 28.32, 26.40, 26.36, 23.18, 23.11, 19.95, 19.54.

Butane-1,2,4-triol (11): ^1H NMR(δ /ppm): 3.64-3.70(m, 1H), 3.62-3.67(t, $J=6.3\text{Hz}$, 2H), 3.40-3.46(m, 2H), 1.50-1.70(m, 2H). ^{13}C NMR(δ /ppm): 69.55, 65.84, 58.60, 35.17.

(4-methyl-tetrahydrofuran-2-yl) methanol (12): *Cis*: ^1H NMR(δ /ppm): 3.91-4.08(m, 2H), 3.31-3.70(m, 3H), 2.29-2.36(m, 1H), 2.05-2.12(m, 1H), 1.24-1.28(m, 1H), 1.04-1.06(d, $J=6.6\text{Hz}$, 3H); ^{13}C NMR(δ /ppm): 80.49, 74.71, 64.97, 35.97, 34.40, 17.70; MS(EI) m/z : 116(M^+ , 57%), 99(100%), 85(69%). *Trans*: ^1H NMR(δ /ppm): 3.91-4.15(m, 2H), 3.31-3.70(m, 3H), 2.30-2.37(m, 1H), 1.81-1.90(m, 1H), 1.51-1.61(m, 1H), 1.03-1.05(d, $J=6.6\text{Hz}$, 3H); ^{13}C NMR(δ /ppm): 79.17, 75.20, 65.23, 35.47, 33.66, 17.70; MS(EI) m/z : 116(M^+ , 72%), 99(100%), 85(62%).

(5-methyl-tetrahydrofuran-2-yl) methanol (13): *Cis*: ^1H NMR(δ /ppm): 4.00-4.10(m, 2H), 3.50-3.65(m, 2H), 1.38-2.20(m, 4H), 1.24-1.27(d, $J=6.0\text{Hz}$, 3H); ^{13}C NMR(δ /ppm): 79.65, 76.10, 65.29, 33.14, 27.29, 21.12; MS(EI) m/z : 116(M^+ , 100%), 99(39%), 85(35%). *Trans*: ^1H NMR(δ /ppm): 4.10-4.20(m, 2H), 3.46-3.72(m, 2H), 1.35-2.30(m, 4H), 1.23-1.25(d, $J=6.0\text{Hz}$, 3H); ^{13}C NMR(δ /ppm): 79.19, 75.35, 65.09, 33.88, 27.80, 20.97; MS(EI) m/z : 116(M^+ , 82%), 99(46%), 85(100%).

2-(5-methyl-tetrahydrofuran-2-yl) propane-2-ol (14): *Cis*: ^1H NMR(δ /ppm): 4.01-4.08(m, 1H), 3.67-3.72(dd, $J=7.5, 7.5\text{Hz}$, 1H), 1.94-2.02(m, 1H), 1.77-1.85(m, 2H), 1.43-1.45(m, 1H), 1.22-1.24(d, $J=6.0\text{Hz}$, 3H), 1.23(s, 3H), 1.14(s, 3H); ^{13}C NMR(δ /ppm): 86.06, 75.63, 71.05, 33.18, 27.31, 26.02, 24.28, 21.20; MS(EI) m/z : 143(M^+-1 , 2%), 127(100%), 111(2%). HRMS calcd for $\text{C}_7\text{H}_{13}\text{O}_2$ ($\text{M}-\text{CH}_3$) $^+$ 129.09155, found 129.09160. *Trans*: ^1H NMR(δ /ppm): 4.07-4.10(m, 1H), 3.81-3.86(dd, $J=9.3, 6.6\text{Hz}$,

1H), 1.94-2.09(m, 2H), 1.80-1.85(m, 1H), 1.47-1.55(m, 1H), 1.22-1.24(d, J=6.0Hz, 3H), 1.23(s, 3H), 1.13(s, 3H); ^{13}C NMR(δ /ppm): 85.43, 76.31, 71.78, 34.58, 27.28, 27.22, 24.00, 21.26; MS(EI) m/z: 143(M^+ -1, 2%), 127(100%), 111(6%). HRMS calcd for $\text{C}_7\text{H}_{13}\text{O}_2$ ($\text{M}-\text{CH}_3$) $^+$ 129.09155, found 129.09161.

2-(5-methyl-5-vinyl-tetrahydrofuran-2-yl)-propane-2-ol (15): Cis: ^1H NMR(δ /ppm): 5.80-6.10(m, 1H), 4.85-5.22(m, 2H), 3.85-3.89(m, 1H), 1.65-1.90(m, 4H), 1.32(s, 3H), 1.23(s, 3H), 1.14(s, 3H); ^{13}C NMR(δ /ppm): 144.29, 111.61, 85.54, 82.81, 71.29, 37.89, 27.36, 26.51, 25.98, 24.30. Trans: ^1H NMR(δ /ppm): 5.80-6.01(m, 1H), 4.90-5.30(m, 2H), 3.79-3.82(m, 1H), 1.65-1.90(m, 4H), 1.32(s, 3H), 1.23(s, 3H), 1.14(s, 3H); ^{13}C NMR(δ /ppm): 143.67, 111.36, 85.54, 83.07, 71.20, 37.44, 27.16, 26.79, 26.32, 24.15.

(2,5-dimethyl-tetrahydrofuran-2-yl) methanol (16): Cis: ^1H NMR(δ /ppm): 4.07-4.20(m, 1H), 3.39-3.49(m, 2H), 1.88-2.00(m, 2H), 1.49-1.65(m, 2H), 1.22-1.24(d, J=6.0Hz, 3H), 1.19(s, 3H); ^{13}C NMR(δ /ppm): 83.19, 74.91, 69.11, 34.15, 34.09, 23.63, 21.25; MS(EI) m/z: 130(M^+ , 12%), 113(100%), 98(40%). Trans: ^1H NMR(δ /ppm): 4.03-4.10(m, 1H), 3.39-3.49(m, 2H), 1.97-2.06(m, 2H), 1.59-1.72(m, 2H), 1.24-1.26(d, J=6.0Hz, 3H), 1.22(s, 3H); ^{13}C NMR(δ /ppm): 83.19, 76.12, 68.55, 33.95, 33.82, 24.69, 21.73; MS(EI) m/z: 130(M^+ , 12%), 113(100%), 98(38%).

(2,5-dimethyl-5-phenyl-tetrahydrofuran-2-yl) methanol (17): Cis: ^1H NMR(δ /ppm): 7.39-7.46(m, 2H), 7.29-7.34(m, 2H), 7.18-7.25(m, 1H), 3.35-3.45(m, 2H), 2.01-2.25(m, 3H), 1.57-1.60(m, 1H), 1.50(s, 3H), 1.36(s, 3H); ^{13}C NMR(δ /ppm): 148.73, 128.30, 126.54, 124.68, 85.29, 68.92, 38.77, 33.42, 31.91, 24.02; MS(EI) m/z: 207(M^+ -1, 2%), 191(8%), 175(100%), 157(33%). HRMS calcd for $\text{C}_{12}\text{H}_{15}\text{O}_2$ ($\text{M}-\text{CH}_3$) $^+$ 191.10720, found 191.10725. Trans: ^1H NMR(δ /ppm): 7.39-7.46(m, 2H), 7.29-7.34(m, 2H), 7.18-7.25(m, 1H), 3.46-3.58(m, 2H), 2.15-2.40(m, 3H), 1.79-1.94(m, 1H), 1.53(s, 3H), 1.20(s, 3H); ^{13}C NMR(δ /ppm): 149.17, 128.00, 126.32, 124.37, 85.25,

69.47, 39.53, 33.97, 31.23, 24.93; MS(EI, m/z): 207(M^+-1 , 2%), 191(7%), 175(100%), 157(31%). HRMS calcd for $C_{12}H_{15}O_2$ ($M-CH_3$)⁺ 191.10720, found 191.10725.

Bistetrahydrofuranyl alcohol (18): Cis: 1H NMR(δ /ppm): 3.92-4.06(m, 2H), 1.50-2.20(m, 8H), 1.30(s, 3H), 1.24(s, 3H), 1.21(s, 3H), 1.12(s, 3H), 1.07(s, 3H); ^{13}C NMR(δ /ppm): 85.55, 84.56, 83.99, 81.25, 72.07, 38.54, 34.40, 28.81, 28.07, 27.93, 27.57, 26.34, 25.24, 24.87. MS(EI): 241(M^+-1 , 4%), 224(67%), 208(8%), 139(100%). Trans: 1H NMR(δ /ppm): 3.78-3.90(m, 2H), 1.55-2.16(m, 8H), 1.25(s, 6H), 1.23(s, 3H), 1.15(s, 3H), 1.12(s, 3H); ^{13}C NMR(δ /ppm): 86.84, 85.75, 84.26, 81.13, 70.75, 38.56, 34.40, 28.62, 28.44, 27.93, 27.66, 26.50, 23.93, 23.35. MS(EI): 241(M^+-1 , 5%), 224(65%), 208(9%), 139(100%).

Bistetrahydrofuranyl alcohol (19): Cis: 1H NMR(δ /ppm): 3.86-4.01(m, 2H), 1.50-2.20(m, 8H), 1.24(s, 9H), 1.15(s, 3H), 1.08(s, 3H); ^{13}C NMR(δ /ppm): 85.67, 84.54, 83.08, 81.17, 72.14, 38.55, 34.59, 28.33, 28.08, 27.77, 27.19, 25.74, 24.97, 24.16. MS(EI): 241(M^+-1 , 5%), 224(52%), 207(10%), 139(100%). Trans: 1H NMR(δ /ppm): 3.78-3.91(m, 2H), 1.65-2.10(m, 8H), 1.25(s, 3H), 1.22(s, 3H), 1.21(s, 3H), 1.16(s, 3H), 1.10(s, 3H); ^{13}C NMR(δ /ppm): 87.07, 83.99, 83.60, 81.07, 70.62, 38.73, 34.44, 28.71, 27.77, 27.67, 27.36, 26.41, 23.99, 23.84. MS(EI) m/z: 241(M^+-1 , 5%), 225(31%), 207(8%), 183(9%), 139(100%).

5-hydroxymethyl-tetrahydro-furan-3-ol (20): Cis: 1H NMR(δ /ppm): 4.30-4.45(m, 2H), 3.40-3.80(m, 4H), 2.18-2.30(m, 1H), 1.71-1.90(m, 1H); ^{13}C NMR(δ /ppm): 78.59, 75.07, 70.81, 63.62, 36.18; MS(EI) m/z: 119(M^++1 , 10%), 101(15%), 87(100%). Trans: 1H NMR(δ /ppm): 4.30-4.45(m, 2H), 3.40-3.80(m, 4H), 2.18-2.30(m, 1H), 1.71-1.90(m, 1H); ^{13}C NMR(δ /ppm): 78.34, 74.66, 71.37, 63.52, 35.94; MS(EI) m/z: 119(M^+ , 12%), 101(15%), 87(100%).

1,5-Bis-hydroxymethyl-tetrahydrofuran (21): Cis: 1H NMR(δ /ppm): 3.90-4.05(m, 2H), 3.60-3.70(m, 2H), 3.38-3.45(m, 2H), 1.78-1.85(m, 2H), 1.60-1.74(m, 2H); ^{13}C

NMR(δ /ppm): 79.56, 64.17, 26.36. **Trans:** ^1H NMR(δ /ppm): 4.00-4.15(m, 2H), 3.55-3.70(m, 2H), 3.40-3.50(m, 2H), 1.91-2.00(m, 2H), 1.59-1.70(m, 2H); ^{13}C NMR(δ /ppm): 80.07, 64.79, 27.49.

References

- [1] W. Wierenga, *The Total Synthesis of Natural Products*, J. Apsimon, Wiley-Interscience: New York, 1981; Vol. 4, pp 287-325
- [2] D. M. Walba and G. S. Stoudt, *Tetrahedron Lett.* 23 (1982) 727.
- [3] T. K. Chakraborty and S. Chandrasekaran, *Tetrahedron Lett.* 25 (1984) 2895.
- [4] M. F. Schlecht and H. Kim, *Tetrahedron Lett.* 26 (1985) 127.
- [5] T. G. Wadell, A. D. Carter and T. J. Miller, *J. Org. Chem.* 57 (1992) 381.
- [6] R. M. Kennedy and S. Tang, *Tetrahedron Lett.* 33 (1992) 3729.
- [7] S. Tang and R. M. Kennedy, *Tetrahedron Lett.* 33 (1992) 5303.
- [8] R. S. Boyce and R. M. Kennedy, *Tetrahedron Lett.* 35 (1994) 5133.
- [9] J. P. Michael, P. C. Ting and P. A. Bartlett, *J. Org. Chem.* 50 (1985) 2416.
- [10] H. M. Ferraz and T. B. Brocksom, *Tetrahedron Lett.* 27 (1986) 811.
- [11] F. E. McDonald and T. B. Towne, *J. Am. Chem. Soc.* 116 (1994) 7921.
- [12] F. E. McDonald and T. B. Towne, *J. Org. Chem.* 60 (1995) 5750.
- [13] T. B. Towne and F. E. McDonald, *J. Am. Chem. Soc.* 119 (1997) 6022.
- [14] S. C. Sinha, A. Sinha, A. Yazbak and E. Keinan, *J. Org. Chem.* 61 (1997) 7640.
- [15] S. C. Sinha and A. Sinha, *J. Am. Chem. Soc.* 119 (1997) 12014.
- [16] Y. Morimoto and T. Iwai, *J. Am. Chem. Soc.* 120 (1998) 1633.
- [17] M. M. Cook and C. Djerassi, *J. Am. Chem. Soc.* 95 (1973) 3678.
- [18] C. Coperet, H. Adolfsson and K. B. Sharpless, *J. Chem. Soc., Chem. Commun.* (1997) 1565.
- [19] J. H. Espenson and M. M. Abu-Omar, *Adv. Chem. Ser.* 253 (1997) 99-134.

- [20] K. P. Gable, *Adv. Organomet. Chem.* 41 (1997) 127-161.
- [21] W. A. Herrmann and F. E. Kühn, *Acc. Chem. Res.* 30 (1997) 169-180.
- [22] C. C. Romão, F. E. Kühn and W. A. Herrmann, *Chem. Rev.* 97 (1997) 3197-3246.
- [23] A. Al-Ajlouni and J. H. Espenson, *J. Am. Chem. Soc.* 117 (1995) 9243-9250.
- [24] A. Al-Ajlouni and J. H. Espenson, *J. Org. Chem.* 61 (1996) 3969-3976.
- [25] H. Tan and J. H. Espenson, *Inorg. Chem.* 37 (1998) 467-472.
- [26] J. Rudolph, K. L. Reddy, J. P. Chiang and K. B. Sharpless, *J. Am. Chem. Soc.* 119 (1997) 6189.
- [27] W. A. Herrmann, R. W. Fischer, M. U. Rauch and W. Scherer, *J. Mol. Catal.* 86 (1994) 243.
- [28] F. A. Carey and R. J. Sundberg, *Advanced Organic Chemistry, Part A, 3rd Ed.*, Plenum Press: New York, 1990.
- [29] C. Paolucci, C. Mazzini and A. Fava, *J. Org. Chem.* 60 (1995) 169-175.
- [30] U. Koert, H. Wagner and U. Pidun, *Chem. Ber.* 127 (1994) 1447-1458.
- [31] M. Zaidlewicz and R. Sarnowski, *Heterocycles* 18 (1982) 281-284.
- [32] Y. Ahn and T. Cohen, *J. Org. Chem.* 59 (1994) 3142-3150.
- [33] E. L. Ghisalberti, E. Twiss and P. E. Rea, *J. Chem. Res. Miniprint* 8 (1991) 1901-1913.
- [34] A. Srikrishna and K. Krishnan, *J. Org. Chem.* 54 (1989) 3981-3983.
- [35] W. Hafner, H. Prigge and J. Smidt, *Justus Liebigs Ann. Chem.* 693 (1966) 109-116.
- [36] W. Shan, P. Wilson, W. Liang and D. R. Mootoo, *J. Org. Chem.* 59 (1994) 7986-7993.
- [37] M. Mischitz, A. Hackinger, I. Francesconi and K. Faber, *Tetrahedron* 50 (1994) 8661-8664.

- [38] K. Mori and P. Puapoomchareon, *Justus Liebigs Ann. Chem.* (1987) 271-272.
- [39] A. Meou, N. Bouanah, A. Archelas, X. M. Zhang, R. Guglielmetti and R. Furtoss, *Synthesis* 9 (1990) 752-753.
- [40] D. Felix, A. Melera, J. Seible and E. Kovats, *Helv. Chim. Acta* 46 (1963) 1513-1532.
- [41] C. Fournier-Nguefack, P. Lhoste and D. Sinou, *Tetrahedron* 53 (1990) 4353-4362.
- [42] A. R. Howell and G. Pattenden, *J. Chem. Soc., Perkin Trans. I* 10 (1990) 2715-2720.
- [43] J. Colonge and G. Clerc, *Bull. Soc. chim. Fr.* 239 (1955) 834.
- [44] R. Paul and S. Tchelitcheff, *Seances Acad. Sci.* 239 (1954) 1504.
- [45] P. Petersson and O. Samulson, *Acta Chem. Scand., Ser. B* 30 (1976) 27.
- [46] M. E. Jung, I. D. Trifunovich and A. W. Sledski, *Heterocycles* 35 (1993) 273-280.

CHAPTER IV

REGIOSELECTIVE HYDROXYLACTONIZATION OF γ,δ -UNSATURATED
CARBOXYLIC ACIDS WITH HYDROGEN PEROXIDE CATALYZED BY
METHYLTRIOXORHENIUM

A paper accepted by *Journal of Molecular Catalysis*

Haisong Tan and James H. Espenson

Abstract

The oxidation of unsaturated carboxylic acids and esters to lactones with hydrogen peroxide is catalyzed by methyltrioxorhenium (MTO). The reaction proceeds regioselectively in high yield. On the basis of the results of this investigation and a comparison with previous work, a concerted process and mechanism have been suggested.

Keywords: Catalysis; Rhenium; Peroxide; Lactonization

1. Introduction

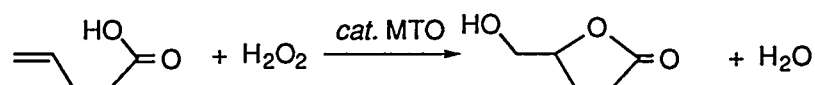
Functionalized γ -lactones serve as chiral building blocks in natural products synthesis [1] and as precursors to HIV-1 protease inhibitors [2, 3]. Many are bioactive natural products [4, 5]. Heteroatom cyclizations lead to γ -lactones; in certain cases this allows two neighboring chiral centers to be introduced selectively and concurrently [6]. Cyclizations of hydroxy acids and esters have been more widely studied, but with unsatisfactory yields [7]. Both β,γ - and γ,δ -unsaturated esters can be oxidized to hydroxy- γ -lactones by the asymmetric dihydroxylation [1].

γ -Lactones have been prepared from unsaturated carboxylic acids with iron porphyrins and iodosylbenzene [6]. Thallium salts induce the lactonization of unsaturated carboxylic acids in ca. 50% yield [8]. *m*-Chloroperbenzoic acid also lactonizes unsaturated carboxylic acids when used with a catalytic amount of Amberlyst-15 ion-exchange resin [9].

We report here a new result: treatment of γ,δ -unsaturated carboxylic acids and esters with H_2O_2 affords δ -hydroxy- γ -lactones in a single, high-yield step at room temperature when methyltrioxorhenium (MTO) is used as a catalyst.

2. Results and Discussion

A convenient and efficient method with H_2O_2 can be used to prepare γ -lactones from the γ,δ -unsaturated carboxylic acids and esters with MTO as the catalyst in chloroform. This method achieves nearly complete regioselectivity with more than 95% yield under mild conditions. The net reaction for the parent 4-pentenoic acid is given by:



Entries 1-3, 5, 7, and 8 in Table 1 illustrate the same reaction for unsaturated carboxylic acids with methyl substituents. Entries 4, 6 and 9 show the products obtained from esters that gave the same lactone products as the acids did. In the first seven entries only a single geometric isomer of the product is possible; the reactions went to 100% conversion with more than 95% selectivity.

As to the mechanism followed, we note that MTO is a well-established catalyst for reactions of hydrogen peroxide [10-12] including the epoxidation of alkenes [13-17] and the oxidative cyclization of hydroxyalkenes [18]. The active forms of MTO are the monoperoxo and diperoxo complexes formed in reversible equilibria:

Table 1. Products of the MTO-catalyzed lactonization reactions.

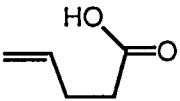
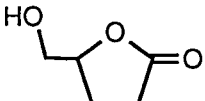
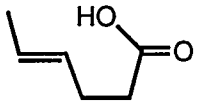
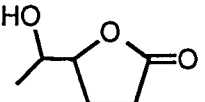
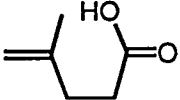
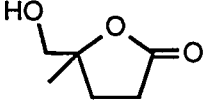
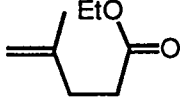
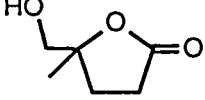
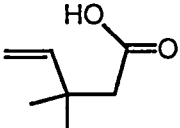
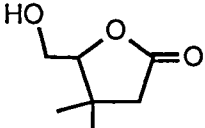
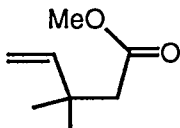
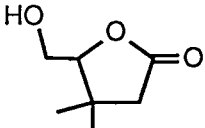
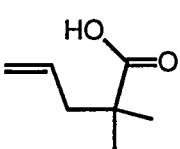
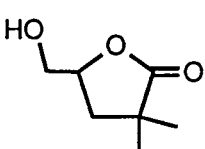
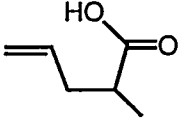
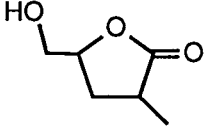
Entry	Reactant	Product (isomer ratio)	Yields (%)	Reaction time (hours)
1			98	14
2			97	9
3			98	9
4		 + EtOH	98	11
5			95	10
6		 + MeOH	95	14
7			98	10
8			97	10
(0.89 : 1.0)				

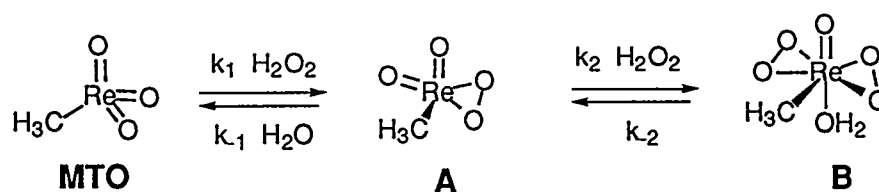
Table 1. (continued)

Entry	Reactant	Product (isomer ratio)	Yields (%)	Reaction time (hours)
9		 + EtOH (0.89 : 1.0)	97	12
10			95	12
11			93	9
12 a			90	8
13 b			80 ^c	10
14			95	9

^a The reaction temperature is 40 °C.

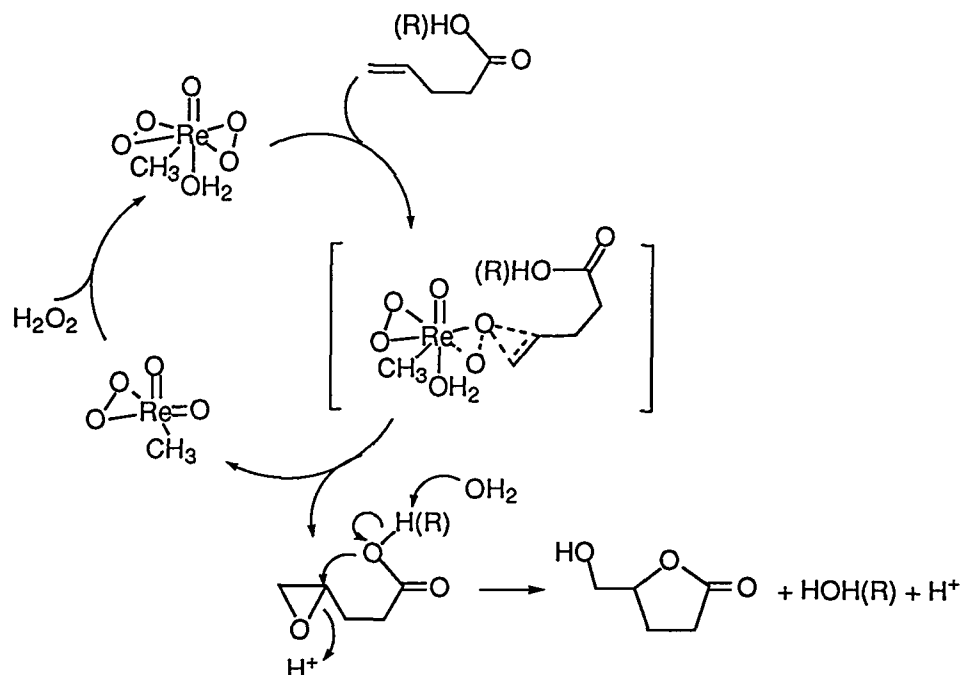
^b solvent: CDCl₃/CD₃CN = 1/1

^c The balance is 5,6-dihydroxyhexanoic acid.



The lactonized products may be formed via the epoxides of the unsaturated carboxylic acids (Scheme 1). The acidic protons that initiate the lactonization of epoxide could come from either the decomposition of MTO or the unsaturated carboxylic acid. The kinetic results did not show any difference between this reaction and the epoxidation reactions that we studied before [13-15]. The hydroxylactonization of the ester was only a little slower than that of the acid. To determine the reaction mechanism of the ester, urea hydrogen peroxide (solid) was used in acetonitrile instead of 30% aqueous hydrogen peroxide [15]. The product of Entry 6 was then the epoxide with ca. 100% yield in 14 h. Then 0.2 M HClO_4 was added to convert epoxide to lactone. This implicates the diol as a possible intermediate for ester hydroxylactonization. The small amount of acid needed for the homogeneous process very likely comes from the decomposition of MTO to perrhenic acid, a strong acid [19]. Alternative sources of acid are the substrate itself, when the acid and not the ester was used, and to the acidic water coordinated to rhenium in compound B. Thus MTO acts as a bifunctional catalyst in this reaction.

The products of Entry 8 were obtained as a mixture of stereoisomers (approximately 0.9:1.0), as determined from the ^1H -NMR spectra, showing an absence of stereochemical control in the reaction. However, these reactions proved to be highly regioselective in that a six-membered ring product was not obtained for lactones 1-11. These substrates all undergo an exo-5-tet cyclization [20]. The very slow cyclization of Entry 12 occurs by an endo-5-tet process.



Scheme 1

After one day, only 30% of the reactant had changed to product. At 40 °C the lactonization reaction was complete in 8 h with a 90% yield.

Entries 13 and 14 were oxidized to tetrahydropyran-2-one. The reaction of 13 was too slow in chloroform, and after two days the product was a mixture of reactant and several products. To increase the solubility of $\text{MTO}-\text{H}_2\text{O}_2$, the binary solvent $\text{CHCl}_3:\text{CH}_3\text{CN}$ (1:1) was used. After nine hours, 6-hydroxymethyl-tetrahydropyran-2-one and 5,6-dihydroxyhexanoic acid were obtained in a 4:1 ratio.

3. Experimental Section

The general procedure used for these catalytic transformations was as follows: MTO (20 μmol) and H_2O_2 (0.50 mmol) in 1.0 mL chloroform was treated with the g,d -unsaturated carboxylic acid (0.40 mmol). The resulting heterogeneous mixture was held at room temperature for 2–20 h, until the ^1H

spectrum revealed the starting compound was absent. Sodium carbonate was then added to decompose MTO. The product was extracted with ether and washed with a small amount of water. ^1H and ^{13}C NMR spectra were obtained from Varian VXR-300 or Bruker DRX-400 spectrometers. Chemical shifts were referenced to Me_4Si . A GC-MS (Varian 3400, Finnegan TSQ 700 triple quadrupole) was used. The spectroscopic data used to identify these products are given in Supporting Information. The stereochemistry was verified from the ^1H -NOE spectra. The ratio of cis and trans isomers was determined by integration of the NMR spectra and from the area of GC peaks.

Acknowledgment. This research was supported by the U. S. Department of Energy, Office of Basic Energy Sciences, Division of Chemical Sciences under contract W-7405-Eng-82.

Supporting Information

Data for the identification of furan and pyran reaction products; NMR (in CDCl_3) and MS data

5-hydroxymethyl-dihydro-furan-2-one (1): ^1H NMR(δ /ppm): 4.61-4.68(m, 1H), 3.88-3.93(dd, $J=12.6$, 2.7Hz, 1H), 3.62-3.68(dd, $J=12.6$, 4.8Hz, 1H), 2.05-2.70(m, 4H); ^{13}C NMR(δ /ppm): 177.94, 80.92, 64.07, 28.72, 23.15; MS(EI): 177(M^++1), 99, 85.

5-(1-hydroxy-ethyl)-dihydro-furan-2-one (2): ^1H NMR(δ /ppm): 4.40-4.43(m, 1H), 4.10-4.13(m, 1H), 2.53-2.61(m, 2H), 2.16-2.27(m, 2H), 1.18-1.20(d, $J=5.1$ Hz, 3H); ^{13}C NMR(δ /ppm): 177.98, 83.74, 67.28, 28.68, 20.93, 17.74; MS(EI): 131(M^++1), 113, 85.

5-hydroxymethyl-5-methyl-dihydro-furan-2-one (3): ^1H NMR(δ /ppm): 3.69-3.49(AB, $J=12$ Hz, 2H), 2.61-2.85(m, 2H), 2.33-2.42(m, 1H), 1.91-1.99(m, 1H), 1.38(s,

3H); ^{13}C NMR(δ /ppm): 177.93, 87.04, 68.27, 29.72, 29.59, 23.07; MS(EI): 130(M^+), 113, 99.

5-hydroxymethyl-4,4-dimethyl-dihydro-furan-2-one (5): ^1H NMR(δ /ppm): 4.17-4.19(m, 1H), 3.80-3.82(m, 2H), 2.32-2.53(m, 2H), 1.22(s, 3H), 1.13(s, 3H); ^{13}C NMR(δ /ppm): 177.11, 88.90, 61.35, 44.18, 38.20, 27.17, 21.64; MS(EI): 144(M^+), 127, 113.

5-hydroxymethyl-3,3-dimethyl-dihydro-furan-2-one (7): ^1H NMR(δ /ppm): 4.56-4.59(m, 1H), 3.87-3.91(dd, $J=12.8$, 3.2Hz, 1H), 3.60-3.64(dd, $J=12.8$, 5.2Hz, 1H), 1.97-2.08(m, 2H), 1.29(s, 6H); ^{13}C NMR(δ /ppm): 182.47, 77.43, 63.65, 40.40, 37.94, 24.83, 24.79; MS(EI): 145(M^++1), 127, 113.

5-hydroxymethyl-3-methyl-dihydro-furan-2-one (8): Cis: ^1H NMR(δ /ppm): 4.49-4.53(m, 1H), 3.89-3.93(m, 1H), 3.64-3.68(m, 1H), 2.72-2.80(m, 1H), 2.33-2.38(m, 1H), 1.73-1.85(m, 1H), 1.29(d, $J=7.2$ Hz, 3H); ^{13}C NMR(δ /ppm): 179.95, 78.58, 64.31, 34.46, 31.64, 16.23; MS(EI): 131(M^++1), 113, 99. Trans: ^1H NMR(δ /ppm): 4.59-4.63(m, 1H), 3.84-3.89(m, 1H), 3.60-3.65(m, 1H), 2.80-2.87(m, 1H), 2.38-2.42(m, 1H), 1.95-2.02(m, 1H), 1.27(d, $J=7.2$ Hz, 3H); ^{13}C NMR(δ /ppm): 180.99, 78.92, 63.53, 35.53, 31.64, 15.12; MS(EI): 131(M^++1), 113, 99.

2,3-dihydroxy-cyclopentaneacetic acid-g-lactone (10): ^1H NMR(δ /ppm): 4.73-4.75(d, $J=6.9$ Hz, 1H), 4.34-4.36(m, 1H), 3.02-3.09(m, 1H), 2.79-2.88(m, 1H), 2.27-2.32(d, $J=13.5$ Hz, 1H), 2.17-2.26(m, 1H), 1.84-1.91(m, 1H), 1.74-1.78(m, 1H), 1.50-1.57(m, 1H); ^{13}C NMR(δ /ppm): 177.86, 90.39, 76.28, 36.19, 35.67, 31.55, 30.80; MS(EI): 143(M^+-1), 125, 84.

5,6-dihydroxybicyclo[2.2.1]-octane-2-carboxylic acid-g-lactone (11): ^1H NMR(δ /ppm): 4.43-4.45(d, $J=5.1$ Hz, 1H), 3.73(s, 1H), 3.15-3.19(m, 1H), 2.49-2.55(dd, $J=11.1$, 4.5Hz, 1H), 2.41-2.42(m, 1H), 2.11-2.15(dd, $J=11.1$, 1.5Hz, 1H), 1.98-2.04(m,

2H), 1.64(m, 1H), 1.59(m, 1H); ^{13}C NMR(δ /ppm): 181.09, 87.22, 77.20, 44.97, 43.50, 38.27, 33.78, 31.64; MS(EI): 155(M^++1), 137, 126, 108.

4-hydroxy-dihydro-furan-2-one (**12**): ^1H NMR(δ /ppm): 4.67-4.72(m, 1H), 4.41-4.46(dd, $J=10.5$, 4.5Hz, 1H), 4.29-4.33(dd, $J=10.5$, 1.2Hz, 1H), 2.73-2.81(dd, $J=18.0$, 6.0Hz, 1H), 2.50-2.57(dd, $J=18.0$, 1.5Hz, 1H); ^{13}C NMR(δ /ppm): 176.07, 76.07, 67.80, 38.00; MS(EI): 103(M^++1), 85.

6-hydroxymethyl-tetrahydro-pyran-2-one (**13**): ^1H NMR(δ /ppm): 4.35-4.40(m, 1H), 3.61-3.66(m, 2H), 2.26-2.53(m, 2H), 1.40-1.90(m, 4H); ^{13}C NMR(δ /ppm): 171.38, 80.23, 63.25, 28.55, 22.65, 17.14; MS(EI): 131(M^++1), 113, 99.

6-(1-hydroxypropyl)-tetrahydro-pyran-2-one (**14**): ^1H NMR(δ /ppm): 4.19-4.26(m, 1H), 3.46-3.53(m, 1H), 2.40-2.89(m, 2H), 1.51-1.97(m, 6H), 0.95-1.02(t, $J=7.5\text{Hz}$, 3H); ^{13}C NMR(δ /ppm): 171.06, 83.04, 74.62, 29.65, 25.58, 24.14, 18.41, 9.91; MS(EI): 159(M^++1), 141, 123.

References

- [1] Z. Wang, X. Zhang and K. B. Sharpless, *Tetrahedron Lett.* 33 (1992) 6407.
- [2] A. K. Ghost, S. P. McKee and W. G. Thompson, *J. Org. Chem.* 56 (1991) 6550.
- [3] D. Askin, M. A. Wallace, J. P. Vacca, R. A. Reamer, R. P. Volante and I. Shinkai, *J. Org. Chem.* 57 (1992) 2771.
- [4] A. E. Wright, M. Schafer, S. Midland, D. E. Munnecke and J. J. Sims, *Tetrahedron Lett.* 30 (1989) 5699.
- [5] M. J. Rieser, J. F. Kozlowski, K. V. Wood and J. L. McLaughlin, *Tetrahedron Lett.* 32 (1991) 1137.
- [6] M. Komuro, T. Higuchi and M. Hirobe, *J. Chem. Soc, Perkin Trans. 1* (1996) 2309.
- [7] B. Simonot and G. Rousseau, *J. Org. Chem.* 59 (1994) 5912.

- [8] H. M. Ferraz and C. M. Ribeiro, *Syn. Commun.* 22 (1992) 399.
- [9] C. W. Jefford and Y. Wang, *J. Chem. Soc., Chem. Commun.* (1987) 1513.
- [10] J. H. Espenson and M. M. Abu-Omar, *Adv. Chem. Ser.* 253 (1997) 99-134.
- [11] W. A. Herrmann and F. E. Kühn, *Acc. Chem. Res.* 30 (1997) 169-180.
- [12] C. C. Romão, F. E. Kühn and W. A. Herrmann, *Chem. Rev.* 97 (1997) 3197-3246.
- [13] A. Al-Ajlouni and J. H. Espenson, *J. Am. Chem. Soc.* 117 (1995) 9243-9250.
- [14] A. Al-Ajlouni and J. H. Espenson, *J. Org. Chem.* 61 (1996) 3969-3976.
- [15] H. Tan and J. H. Espenson, *Inorg. Chem.* 37 (1998) 467-472.
- [16] J. Rudolph, K. L. Reddy, J. P. Chiang and K. B. Sharpless, *J. Am. Chem. Soc.* 119 (1997) 6189.
- [17] W. A. Herrmann, R. W. Fischer, M. U. Rauch and W. Scherer, *J. Mol. Catal.* 86 (1994) 243.
- [18] H. Tan and J. H. Espenson, (1998) submitted for publication.
- [19] M. Abu-Omar, P. J. Hansen and J. H. Espenson, *J. Am. Chem. Soc.* 118 (1996) 4966-4974.
- [20] J. E. Baldwin, *J. Chem. Soc., Chem. Commun.* (1976) 734.

CHAPTER V

THE BASE HYDROLYSIS OF METHYLTRIOXORHENIUM: THE MECHANISM
REVISED AND EXTENDED: A NOVEL APPLICATION OF ELECTROSPRAY
MASS SPECTROMETRY

A paper published in *Inorganic Chemistry* *

James H. Espenson*, Haisong Tan, Sahana Mollah, R. S. Houk, and Matthew D. Eager

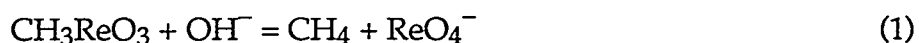
Abstract.

The full kinetic pH profile for the base-promoted decomposition of MTO to CH₄ and ReO₄⁻ was examined with the inclusion of new data at pH 7–10. Spectroscopic and kinetic data gave evidence for mono- and di-hydroxo complexes: MTO(OH⁻) and MTO(OH⁻)₂. Parallel unimolecular eliminations of methane from these species account for the rate–pH profile; the respective rate constants are: MTO(OH⁻), $k = 4.56 \times 10^{-5} \text{ s}^{-1}$ and MTO(OH⁻)₂, $k = 2.29 \times 10^{-4} \text{ s}^{-1}$ at 25 °C. Some kinetic data were acquired with electrospray mass spectrometry to monitor the buildup in the concentration of perrhenate ions. Reliable signals for each of the isotopomers of ReO₄⁻ were obtained by this method with initial MTO concentrations of 160 μM.

* Espenson, J. H.; Tan, H; Mollah, S; Houk, R. S. *Inorg. Chem.* **1998**, *37*, 4621.

Introduction

The base hydrolysis kinetics of methyltrioxorhenium (CH_3ReO_3 , abbreviated as MTO) was reported by two groups of workers in 1996.^{1,2} Both groups, agreeing that the exclusive products are methane and perrhenate ions, wrote this chemical equation for the net reaction:



The pH ranges of the two investigations were, however, widely separated, approximately 3-6¹ and 11-14². Neither set of data can correctly be extrapolated to the intermediate pH region while also supporting the independent claims as to mechanism. The dilemma in the kinetics is clearly apparent from the two pieces of the experimental pH profile, shown in Figure 1. Both sets of data are shown as solid lines within the pH region actually measured, using the analytical expressions for the rate constants to construct these curves. Additionally, the rate law from each set of experiments was then extrapolated toward neutral pH, outside the range of measurement, by the mathematical forms given in the respective reports. The extrapolated curves diverge widely. Both interpretations cannot be as stated: the rate constants thus assigned could not be reconciled with one another, in that they differ by more than four orders of magnitude. Expressed as the value of k in the equation $v = k[\text{MTO}][\text{OH}^-]$, the respective values of k are $8.6 \times 10^2 \text{ L mol}^{-1} \text{ s}^{-1}$ (extrap. to 298 K)¹ vs. $2.7 \times 10^{-2} \text{ L mol}^{-1} \text{ s}^{-1}$.² Neither set of data *necessarily* disagrees with the other, however, if a more refined model can be formulated on the basis of kinetics in the intermediate pH range. The goal of this study has been to obtain kinetic data that cover the full pH range and to formulate a single mechanism to describe all the data.

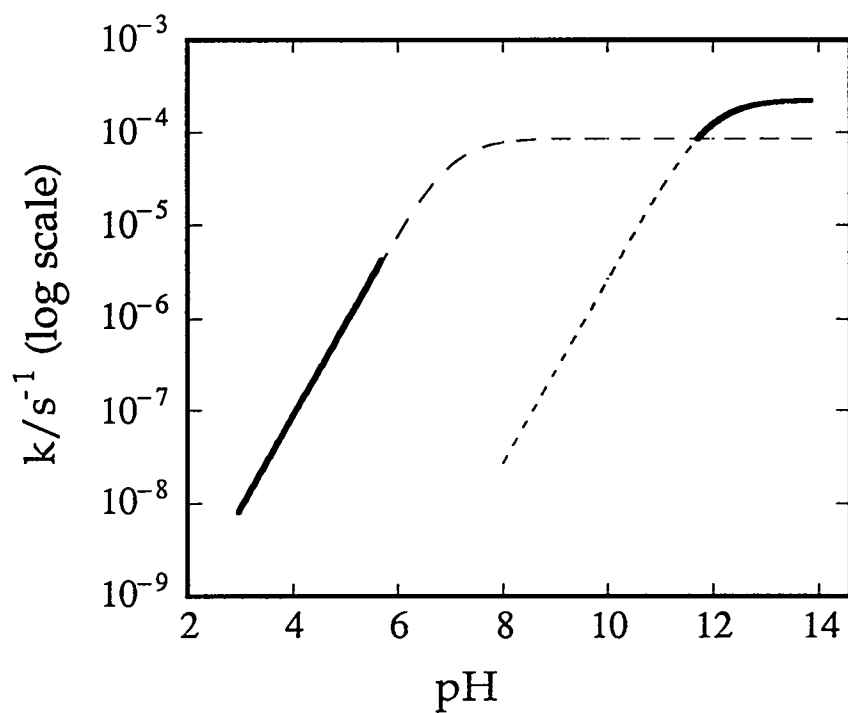


Figure 1. The pH profiles for two sets of kinetic data for the OH^- -induced decomposition of MTO. One set used data for pH 2.97–5.70, extrapolated to 25 $^{\circ}\text{C}$,¹ the other set refers to measurements over the range 11.7–13.8. Each is shown as a bold line. Each set of data was extrapolated by the chemical and algebraic model given in the respective publication, with the extrapolated portions shown as dashed lines.

The reaction kinetics has now been studied at intermediate pH values, with UV-Vis and electrospray mass spectrometric (ES-MS) techniques. The ES-MS technique is widely used for the determination of the molecular weights and structures of large biological molecules.^{3,4} This technique has also been used for the determination of many inorganic species, from ion clusters to bare metal ions.⁵⁻¹⁰ To date, applications of the ES-MS method to kinetics problems have, however, been relatively rare.⁷

Experimental Section

Materials. The solutions for kinetics were prepared using high-purity water obtained by passing laboratory distilled water through a Millipore-Q water purification system. HPLC-grade acetonitrile (Fisher Scientific) was used in the ES-MS measurements. MTO, sodium perrhenate, sodium para-toluenesulfonate (= tosylate), sodium carbonate, and potassium phosphate were used as received.

Instrumentation. UV-Vis spectra were obtained from a Shimadzu UV-3101PC instrument. A Perkin-Elmer SCIEX API-1 mass spectrometer was used for the ES-MS study. Typical conditions used in the operation of the ES-MS instrumentation are summarized in Table 1. The voltages were optimized to maximize the signal for the species of interest. Peak hopping data were collected using a 100-ms dwell time. Spectral scans were collected by adding ten consecutive scans together using a dwell time of 10 ms per 0.1 amu.

Kinetics. All of the kinetics determinations, by the UV and ES-MS methods, were carried out in aqueous solution at 25.0 ± 0.5 °C. A 5 cm quartz cuvette was used, and the starting concentration of MTO was 1.60×10^{-4} M (40 ppm).

Table 1. Typical ES-MS operating conditions

Sample flow rate	17 $\mu\text{L min}^{-1}$
Nebulizer gas, pressure	Nitrogen, 280 kPa
Curtain gas, back pressure, temperature	Nitrogen (ultra pure carrier grade), 550 kPa, 45 °C
Ionization needle voltage (V_{ISV})	−4400 V
Interface plate voltage (V_{IN})	−450 V
Orifice plate voltage (V_{OR})	−130 V
RF only quadrupole voltage (V_{RO})	−100 V
Mass analyzer quadrupole voltage (V_{RI})	−95 V
CEM detector voltage	2500 V
Operating pressure of quadrupole chamber	4.0 mPa

Other concentrations were 3.09×10^{-5} M (6 ppm) sodium tosylate, and 1–20 mM buffer solution. The solution was diluted with an equal volume of acetonitrile just before the ES-MS measurement. The addition of an organic solvent greatly enhances the ion signal in ES-MS. The actual kinetics data apply, however, to a strictly aqueous medium. The buffers used for the different pH ranges were: 4.5–6.0, HOAc/NaOAc; 6.5–8.0, $\text{KH}_2\text{PO}_4/\text{K}_2\text{HPO}_4$; and 8.0–10.5, $\text{NaHCO}_3/\text{Na}_2\text{CO}_3$. Above pH 10.5, NaOH alone determined the pH. The ionic strength change proved to have little influence on the rate constants

Results

Kinetics. As will be shown, data in the intermediate pH region do define an approximate plateau between the limiting values of the earlier studies,

although the rate constants are not those that would have been extrapolated from either of the previous experimental studies. We can now propose a mechanism to account for the kinetic data over the entire pH range.

The decomposition of MTO to perrhenate ions was followed at several UV wavelengths. Some reactions were followed by monitoring the absorbance as a function of time at a fixed wavelength; the readings would rise or fall with time depending on the relative values of the molar absorptivities of MTO and ReO_4^- at the chosen wavelength. Other experiments were based on repetitive UV scans over time. In one treatment, these files were analyzed by extracting absorbance values at a given wavelength. In both of these cases the rate constant was obtained by nonlinear least-squares fits to a first order rate equation: $\text{Abs}_t = \text{Abs}_\infty + (\text{Abs}_0 - \text{Abs}_\infty) \times \exp(-kt)$. The single-wavelength data were of greater precision, however, and were used in this analysis.

ES-MS has been used for the determination of many inorganic ions both qualitatively and quantitatively.¹¹ We have found that the perrhenate anion gives a clean mass spectrum in 1:1 $\text{CH}_3\text{CN}:\text{H}_2\text{O}$ solution under ES-MS conditions. The only two significant peaks are those for the two isotopes, ^{185}Re and ^{187}Re , with natural abundances of 37.07% and 62.93%, respectively.¹² Thus ReO_4^- shows peaks at m/z 249 and 251 in a relative abundance of 1:1.7. Using the tosylate anion (m/z 171) as the internal standard for concentration, we were able to monitor the increase in intensity of each of the perrhenate peaks with time as the reaction proceeded at pH 7–10.

Figure 2 shows the change in the perrhenate signal at m/z 251, relative to tosylate, as a function of time. The time to collect the mass spectral data was ~ 100 s, which is much smaller than the reaction time, typically $\sim 10^4$ s. The intensity-

time data gave excellent fits to first-order kinetics. Errors are standard deviations estimated from counting statistics based on total counts observed for each species.

To determine the absolute conversion in the decomposition reaction, the method of standard additions was applied. Under the same ES-MS conditions, increments of a sodium perrhenate solution were added to the reaction vessel at concentrations 4–16 ppm in total. This was done to spent reaction solutions at pH 7 and 10. Figure 3 shows this result at pH 10. There is a nearly linear increase of the intensity ratio with the concentration of the added perrhenate ions. If this line is extrapolated linearly to the abscissa, its intercept corresponds to a value of 22 ppm of ReO_4^- . This is only slightly higher than that of the nominal value of 20 ppm, which could be due to the volume contraction upon mixing water and acetonitrile.

pH Variation. The various buffers listed previously were used to set $[\text{OH}^-]$ in different experiments in the pH range 5–11. Since MTO was present in the range $(1\text{--}2) \times 10^{-4}$ M, much lower than the buffer capacity, the pH could be taken as nearly constant in each experiment. The new kinetic data, from UV and ES-MS, along with the experimental data at low pH¹ and high pH,² were used to create a new pH profile, given in Figure 4.

Interpretation and Discussion

Mechanisms. The pH profile shows two rising portions and two plateaus, as if the data represented the titration curves for the formation of two intermediates. Indeed, this concept provides the basis for one of the mechanisms that can be drawn to account for the pH profile. The acidity of MTO (pK_a 7.5)^{13,14} has been recognized, which we find convenient to write as the complexation of OH^- :

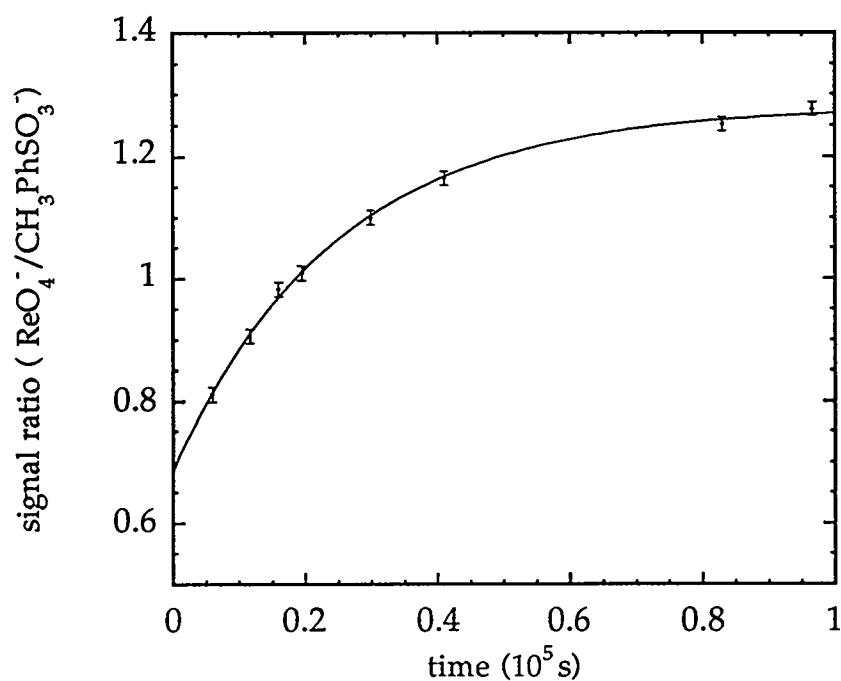


Figure 2. A typical plot of the signal ratio for $\text{ReO}_4^-/\text{TsO}^-$ vs time obtained in an ES-MS experiment. The initial concentration of MTO was 160 μM and the pH was buffered at 8.0. The curve shown corresponds to one of the two isotopes of rhenium. The curves through the points are the first-order kinetic fits.

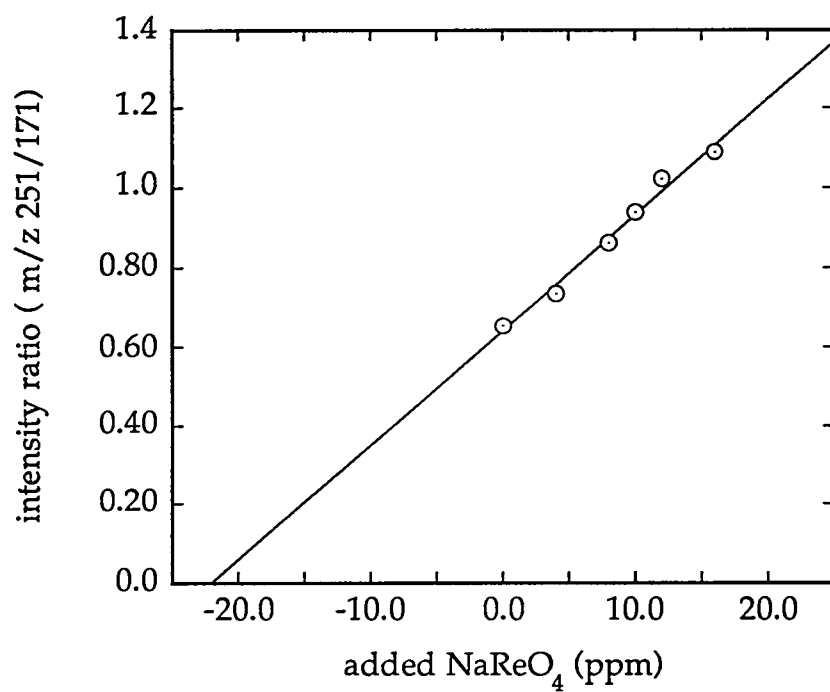


Figure 3. The standard addition plot used to determine the final concentration in an ES-MS experiment. The initial MTO concentration was 20 ppm, and the final perrhenate concentration, given by the x-intercept, is 22 ppm.

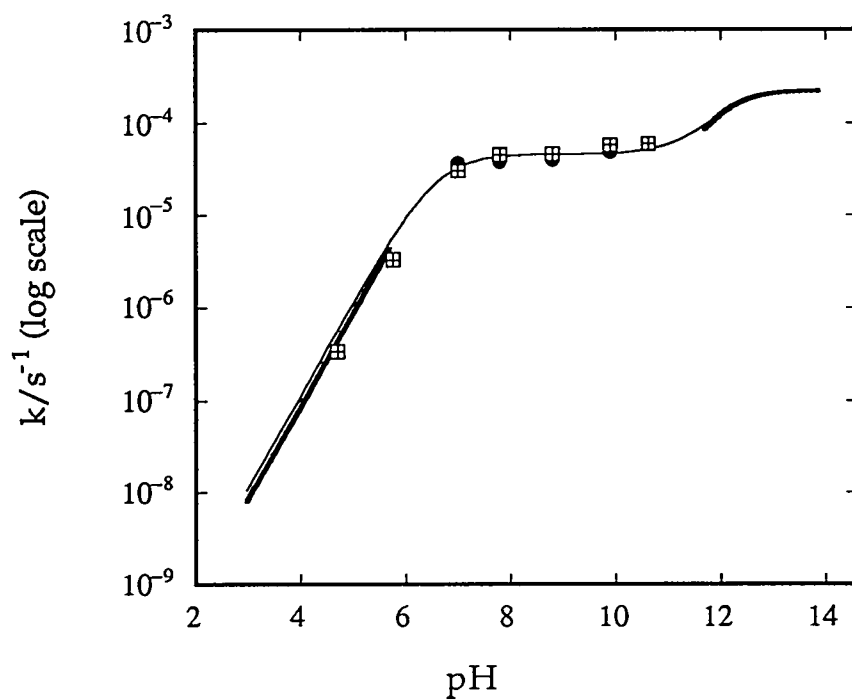
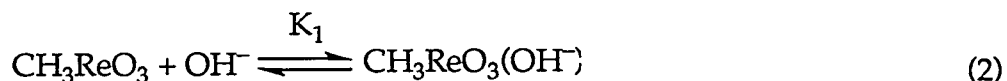
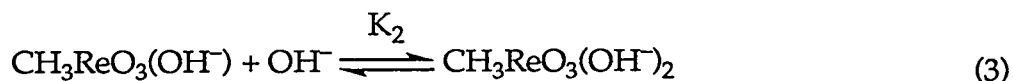


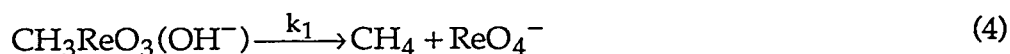
Figure 4. The variation of the observed rate constant with pH, including the new values at intermediate pH, shown as O (ES-MS) and X (UV-Vis). The solid curve is the fit of all data to eq 6.



If the second, high-pH plateau is to be accounted for in an analogous manner, then a second equilibrium, eq 3, must be written:



If this is the model, then each species must react independently at the unimolecular rate given by its plateau. The chemical equations are as shown in eq 4 and 5:



The smooth curve in **Figure 4** is the pH profile for the fit of the rate constants to this model, as expressed in the equation

$$k = \frac{k_1 K_1 [\text{OH}^-] + k_2 K_1 K_2 [\text{OH}^-]^2}{1 + K_1 [\text{OH}^-] + K_1 K_2 [\text{OH}^-]^2} \quad (6)$$

In the low-pH region, the rate is $k_1 K_1 [\text{OH}^-]$, in agreement with the form reported.¹ In the limit of very high pH, the rate will be given by $k_2 K_2 [\text{OH}^-] / (1 + K_2 [\text{OH}^-])$, also consistent with the form reported.²

The data over the entire pH range were fitted by eq 6 using the method of nonlinear least-squares regression, and the four parameters deduced without reference to values reported previously. The fitted values of the parameters are:

$$k_1 = 4.56 \pm 0.20 \times 10^{-5} \text{ s}^{-1} \quad K_1 = 2.5 \pm 0.9 \times 10^7 \text{ L mol}^{-1}$$

$$k_2 = 2.29 \pm 0.03 \times 10^{-4} \text{ s}^{-1} \quad K_2 = 73.1 \pm 5.6 \text{ L mol}^{-1}$$

Let us now examine what comparisons can be made on the basis of these values. The value of K_1 affords $\text{pK}_{\text{a}1} = 6.70$, perhaps acceptably close to the reported 7.5, given the different methods employed. From K_2 and $\text{pK}_{\text{w}} = 14$, $\text{pK}_{\text{a}2} = 12.2$ for $\text{MTO}(\text{OH}^-) + \text{H}_2\text{O} = \text{MTO}(\text{OH}^-)_2 + \text{H}^+$; this compares favorably with the reported value,² $\text{pK}_{\text{a}} = 11.9$ (kinetics) and 11.7 (UV titration) under alkaline conditions. Of course the symbolism used in this work is different than that in Ref. 2, and this constant is not labeled the same there as it appears here.

From the calculated product k_1K_1 , we have the apparent bimolecular rate constant for the reaction of $\text{MTO} + \text{OH}^-$ in the acidic region: $1.03 \times 10^3 \text{ L mol}^{-1} \text{ s}^{-1}$, compared to $0.86 \times 10^3 \text{ L mol}^{-1} \text{ s}^{-1}$, calculated from the kinetic data and the value of K_1 . The difference is not large and can be traced to the ways in which $\text{pK}_{\text{a}1}$ was treated.

What is one to make of the unimolecular constants cited above: $k_1 = (4.56 \pm 0.20) \times 10^{-5} \text{ s}^{-1}$ and $k_2 = (2.29 \pm 0.03) \times 10^{-4} \text{ s}^{-1}$? The two are similar to one another, being separated by a factor of only 5. In contrast, MTO itself shows no tendency to produce methane. These findings imply that the reaction occurs by the elimination of methane from the methyl group and the proton of the coordinated hydroxide. Whether one OH^- group or two are coordinated to rhenium makes rather little difference; at most, the second hydroxide facilitates methane release by making the incipient perrhenate ion into a better leaving group.

Independent evidence has been obtained for each of the hydroxo-MTO anions. The bright yellow $[\text{MTO}(\text{OH})_2]^-$ was detected spectrophotometrically and is also evident from pH measurements.^{13,14} The UV-Vis spectra of MTO remains the same between pH 1 and 6, whereas it changes above pH ~6 and ~11. These

findings and the shape of the pH titration curve provide support for the species $[\text{MTO}(\text{OH})]^-$ and $[\text{MTO}(\text{OH})_2]^{2-}$.

The electrospray conditions that produced strong signals for perrhenate and tosylate ions did not show the presence of $[\text{MTO}(\text{OH})]^-$ or $[\text{MTO}(\text{OH})_2]^{2-}$. This at first appeared alarming, since $[\text{MTO}(\text{OH})]^-$ should be present at a significant concentration at pH 8–11 according to our analysis, Figure 5. When the voltage difference between the skimmer and the RF-only quadrupole rods was reduced from 30 V to 3 V, weak peaks of $[\text{MTO}(\text{OH})\cdot 4\text{H}_2\text{O}]^-$ became evident in the spectrum at pH 11 in a carbonate buffer. Apparently, collision conditions that are energetic enough to strip solvent molecules from $[\text{MTO}(\text{OH})\cdot 4\text{H}_2\text{O}]^-$ also cause it to disproportionate. This solvated anion would have been missed had the measurements been restricted to a single collision energy, illustrating the importance of examining the effect of collision conditions on electrospray spectra of inorganic and organometallic ions before concluding the certain species are absent from the sample, as noted by others.^{5,8-10}

The secondary solvation of this anion was found under these conditions, because of the low energy used. A further finding emerged: an additional peak corresponding in mass to "MeReO₅⁻" was seen, but only in carbonate buffer. The point was not investigated further, perhaps in alkaline solution MTO catalyzes the conversion of CO_3^{2-} to CO_2 .

Figure 5 shows the constructed speciation diagram for MTO and its hydroxo complexes, calculated from the best-fit values of K_1 and K_2 . Recognition of the species present over the entire range allows the formulation of a satisfactory mechanism.

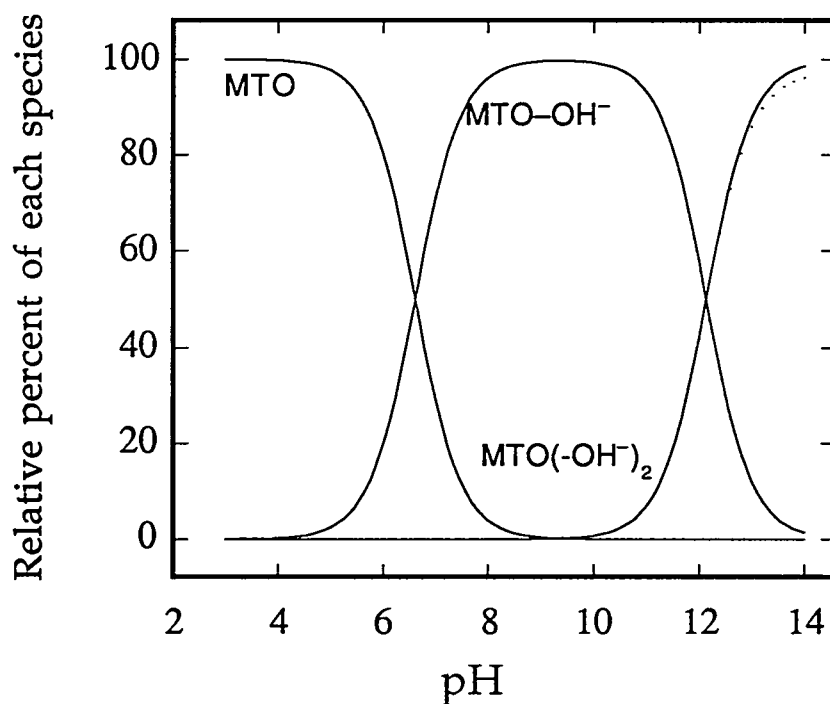


Figure 5. The speciation diagram for MTO and its hydroxo complexes, determined from the fitted values of K_1 and K_2 .

This appears to be one of the early applications, and perhaps the first, of the ES-MS technique to a kinetics problem in inorganic or organometallic chemistry. The exceptional sensitivity of the method should commend it for many applications.

Acknowledgment. This research was supported by the U. S. Department of Energy, Office of Basic Energy Sciences, Division of Chemical Sciences under contract W-7405-Eng-82.

References

- (1) Laurenczy, G.; Lukács, F.; Roulet, R.; Herrmann, W. A.; Fischer, R. W. *Organometallics* **1996**, *15*, 848-851.
- (2) Abu-Omar, M.; Hansen, P. J.; Espenson, J. H. *J. Am. Chem. Soc.* **1996**, *118*, 4966-4974.
- (3) Fenn, J. B.; Mann, M.; Meng, C. K.; Wong, S. F.; Whitehouse, C. M. *Science* **1989**, *246*, 46.
- (4) Smith, R. D.; Loo, J. A.; Edmonds, C. G.; Barinaga, C. J.; Udseth, H. R. *Anal. Chem.* **1990**, *62*, 882.
- (5) Colton, R.; D'Agostino, A.; Traeger, J. C. *Mass Spectrom. Rev.* **1995**, *14*, 79.
- (6) Corr, J. J.; Anacleto, J. F. *Anal. Chem.* **1996**, *68*, 2155.
- (7) Charbonniere, L. J.; Williams, A. F.; Frey, U.; Merbach, A. E.; Kamalaprija, P.; Schaad, O. J. *Am. Chem. Soc.* **1997**, *119*, 2488-2496.
- (8) Blades, A. T.; Jayaweera, P.; Ikonomou, M. G.; Kebarle, P. J. *J. Phys. Chem.* **1990**, *92*, 5900.
- (9) Blades, A. T.; Ho, Y.; Kebarle, P. J. *J. Phys. Chem.* **1996**, *100*, 2443.
- (10) Klassen, J. S.; Kebarle, P. J. *J. Am. Chem. Soc.* **1996**, *118*, 12437.
- (11) Guizdala, A. B., III; Johnson, S. K.; Mollah, S.; Houk, R. S. *Anal. Atom. Spectro.* **1997**, *12*, 503.
- (12) Friedlander, G.; Kennedy, J. W. ; John Wiley & Sons, Inc: New York, 1955, p p 434.
- (13) Herrmann, W. A.; Fischer, R. W.; Scherer, W. *Adv. Mater.* **1992**, *4*, 653.
- (14) Herrmann, W. A.; Fischer, R. W. *J. Am. Chem. Soc.* **1995**, *117*, 3223.

GENERAL CONCLUSIONS

The rate control step of MTO-catalyzed silane oxidation involves electrophilic attack by bisperoxide rhenium B on the Si-H bond. The Si-H stretching is important in the rate-determining step, with the stronger bonds (those of higher frequency) possessing less reactivity. The dimerization of silanol can be catalyzed by the trace acid which comes from the decomposition of MTO. So when UHP is used instead of 30% hydrogen peroxide water solution, silanol are obtained with high yield. The difference of the activation energy between experiment and calculation data comes from the solvent effect.

Conjugated diene can be oxidized by $\text{H}_2\text{O}_2/\text{MTO}$. The MTO-catalyzed epoxidations are controlled in rate by the electron density at the double bond and by the extent of conjugation of the double bonds. The primarily-produced epoxide is that at the most electron-rich of the double bonds. Epoxides are obtained when urea-hydrogen peroxide (UHP) is used instead of hydrogen peroxide, since the activity of water is low and the epoxide undergoes a slow ring-opening reaction.

The oxidation of 5-hydroxyalkenes by $\text{H}_2\text{O}_2/\text{MTO}$ leads to functionalized tetrahydrofurans. In these cases no tetrahydropyrans was formed. The results show that the first reaction between the substrate and a bisperoxide B ($\text{CH}_3\text{Re}(\text{O})(\text{H}_2\text{-O}_2)_2(\text{H}_2\text{O})$) yields an epoxide. This intermediate was not detected because cyclization occurred so rapidly. 6-Hydroxyalkenes were similarly but more slowly converted to tetrahydropyran alcohols.

Both unsaturated carboxylic acids and esters can be regioselectively oxidized to lactones with hydrogen peroxide catalyzed by MTO. In these reactions MTO acts as a bifunctional catalyst for both epoxidation and cyclization. Five and six-member ring lactones can be formed during the cyclization reactions.

The full kinetic pH profile for the base-promoted decomposition of MTO to CH_4 and ReO_4^- shows two rising portions and two plateaus, which implies the formation of two intermediates. Spectroscopic and kinetics data gave evidence for mono- and dihydroxo complexes: $\text{MTO}(\text{OH}^-)$ and $\text{MTO}(\text{OH}^-)_2$. Parallel unimolecular eliminations of methane from these species account for the rate-pH profile. Some kinetic data were acquired with electrospray mass spectrometry to monitor the build up in the concentration of perrhenate ions. This appears to be one of the early applications, and perhaps the first, of the ES-MS technique to a kinetics problem in inorganic or organometallic chemistry.

ACKNOWLEDGMENTS

I would like to express my deep appreciation to Professor James H. Espenson for his guidance, support and encouragement during my graduate study. I am also thankful for Professor Robert S. Houk who guides me in analytical chemistry, especially in electrospray mass spectrometry.

Thanks are also extended to the members of my research group, both past and present. In particular, I would like to thank Dr. Andreja Bakac and Dr. Weidong Wang for their help and useful discussions.

I would also like to thank Sahana Mollah for the electrospray mass measurement and Professor Mark S. Gordon and Dr. Akihiko Yoshikawa for the theoretical calculations.

I especially thank my wife Ren for her continuous caring, inspiring, and understanding me in every aspect of my life.

This work was performed at Ames Laboratory under Contract No. W-7405-Eng-82 with the U. S. Department of Energy. The United States government has assigned the DOE Report number IS-T 1882 to this thesis.